



Filer, D., Thompson, M. A., Takhaveev, V., Dobson, A. J., Kotronaki, I., Green, J. W.M., Heinemann, M., Tullet, J. M.A. and Alic, N. (2017) RNA polymerase III limits longevity downstream of TORC1. *Nature*, 552(7684), pp. 263-267.

There may be differences between this version and the published version. You are advised to consult the publisher's version if you wish to cite from it.

<http://eprints.gla.ac.uk/203079/>

Deposited on: 12 November 2019

Enlighten – Research publications by members of the University of Glasgow
<http://eprints.gla.ac.uk>

Longevity by RNA polymerase III inhibition downstream of TORC1

Danny Filer¹, Maximillian A. Thompson², Vakil Takhaveev³, Adam J. Dobson¹, Ilektra
Kotronaki¹, James W.M. Green², Matthias Heinemann³, Jennifer M.A. Tullet² and
Nazif Alic¹

¹Institute of Healthy Ageing, Department of Genetics, Evolution and Environment,
University College London, Gower St, London, WC1E 6BT, UK.

²School of Biosciences, University of Kent, Canterbury, CT2 7NJ, UK.

³Molecular Systems Biology, Groningen Biomolecular Sciences and Biotechnology
Institute, University of Groningen, 9747 AG, Groningen, Netherlands.

Summary

Three distinct RNA polymerases (Pols) transcribe different classes of genes in the eukaryotic nucleus¹. Pol III is the essential, evolutionarily conserved enzyme that generates short, non-coding RNAs, including transfer RNAs (tRNAs) and 5S ribosomal RNA (rRNA)². Historical focus on transcription of protein-coding genes has left the roles of Pol III in organismal physiology relatively unexplored. The prominent regulator of Pol III activity, Target of Rapamycin kinase Complex 1 (TORC1), is an important longevity determinant³, raising the question of Pol III's involvement in ageing. Here we show that Pol III limits lifespan downstream of TORC1. We find that a reduction in Pol III extends chronological lifespan in yeast and organismal lifespan in worms and flies. Inhibiting Pol III activity in the adult worm or fly gut is sufficient to extend lifespan, and in flies, longevity can be achieved by Pol III inhibition specifically in the intestinal stem cells (ISCs). The longevity phenotype is associated with amelioration of age-related gut pathology and functional decline, dampened protein synthesis and increased tolerance of proteostatic stress. Importantly, Pol III acts downstream of TORC1 for lifespan and limiting Pol III activity in the adult gut achieves the full longevity benefit of systemic TORC1 inhibition. Hence, Pol III is a pivotal output of this key nutrient signalling network for longevity; Pol III's growth-promoting, anabolic activity mediates the acceleration of ageing by TORC1. The evolutionary conservation of Pol III affirms its potential as a therapeutic target.

Main text

The labour of transcription in the eukaryotic nucleus is divided amongst Pol I, II and III^{1,4}. This specialisation is evident in the biogenesis of the translation machinery, a task for which all three Pols are co-ordinately required: Pol I generates the 45S pre-rRNA that is subsequently processed into mature rRNAs, Pol II transcribes various RNAs including messenger RNAs (mRNAs) encoding ribosomal proteins (RPs), while Pol III provides the tRNAs and 5S rRNA. To match the extrinsic conditions and the intrinsic need for protein synthesis, this costly process of generating protein synthetic capacity is tightly regulated by the key driver of cellular anabolism: TORC1^{5,6}. The central position of TORC1 in the control of fundamental cellular processes is mirrored by the striking impact of its activity on organismal physiology: following the initial discovery in worms⁷, the inhibition of TORC1 has been demonstrated to extend lifespan in all organisms tested, from yeast to mice^{8,9}, with beneficial effects on a range of age-related diseases and dysfunctions^{3,10}. TORC1 strongly activates Pol III transcription^{5,6} and this relationship suggests the possibility that inhibition of Pol III promotes longevity. Here, we test this hypothesis.

In *S. cerevisiae*, each of the 17 Pol III subunits is encoded by an essential gene. We generated a yeast strain in which its largest subunit (C160, encoded by *RPC160/RPO31*⁴) is fused to the auxin-inducible degron (AID). The fusion protein can be targeted for degradation by the ectopically expressed E3 ubiquitin ligase (OsTir) in the presence of indole-3-acetic acid (IAA)¹¹ to achieve conditional inhibition of Pol III (**Extended Data Fig. 1a**). We confirmed that IAA treatment triggered the degradation of the fusion protein (**Fig. 1a**) and observed IAA improve the survival of the *RPC160-AID* strain upon prolonged culture (**Fig. 1b**). In addition, IAA treatment of the control strain lacking the AID fusion reduced its survival, relative to same strain in absence of

IAA and the *RPC160-AID* strain in presence of IAA (**Extended Data Fig. 1b**). Hence, Pol III depletion appears to extend yeast chronological lifespan. Note that IAA had no substantial effect on the survival of a strain carrying the AID domain fused to the largest subunit of Pol II (*RPB220-AID*), which appeared to survive better than the control strain in the presence of IAA (**Extended Data Fig. 1a and b**), indicating inhibition of Pol II may also extend chronological lifespan. Yeast chronological lifespan is a measure of survival in a nutritionally-limited, quiescent population. Replicative lifespan, on the other hand, measures the number of daughters produced by a single mother cell in its lifetime. We found no evidence that inhibition of Pol III causes an increase in yeast replicative lifespan (**Extended Data Fig. 1c**).

The observed increase in yeast chronological lifespan may simply be indicative of increased stress resistance and hence bear limited relevance to organismal ageing. To examine the role of Pol III in organismal ageing directly, we turned to animal models. We treated *C. elegans* from the L4 stage with RNAi against *rpc-1*, the worm orthologue of *RPC160*, achieving a partial knockdown of its mRNA (**Fig. 1c**). This consistently extended worm lifespan at both 20°C and 25°C (**Fig. 1d; Extended Data Fig. 2a and b**, see **c** for summary of worm lifespans). To reduce Pol III activity in the fruit fly, we backcrossed a P-element insertion deleting the transcriptional start site of the gene encoding the Pol III-specific subunit C53 (*CG5147^{EY22749}*, henceforth called *dC53^{EY}*, **Extended Data Fig. 3**) into a healthy, outbred *D. melanogaster* population. Homozygous *dC53^{EY/EY}* mutants were not viable but heterozygous females had a partial reduction in *dC53* mRNA and lived longer than controls (**Fig. 1e and f**; see **Extended Data Fig. 4a** for summary of fly lifespans). Taken together, our data strongly indicate that Pol III limits lifespan in multiple model organisms and, conversely, that partial inhibition of its activity is an evolutionarily conserved longevity intervention.

The longevity of an animal can be governed from a single organ. In the worm, this role is often played by the gut^{12,13}. To restrict the *rpc-1* knock-down to the gut, we used *rde-1* null worms whose RNAi machinery deficiency is restored solely in the gut by gut-specific *rde-1* rescue¹⁴. *rpc-1* RNAi extended the lifespan of this strain, both at 20°C and 25°C (**Fig. 2a, Extended Data Fig. 2d**). Similarly, in the adult fly, driving an RNAi construct targeting the *RPC160* orthologue (*CG17209*, henceforth called *dC160*, **Extended Data Fig. 3**) with the mid-gut-specific, RU486-inducible driver (*TIGS*) extended female lifespan (**Fig. 2b**), while the presence of the inducer (RU486) did not affect survival of the control lines (**Extended Data Fig. 4b and c**). The longevity phenotype could also be recapitulated with RNAi against another Pol III subunit (*dC53*, **Extended Data Fig. 4d**), indicating it is not due to off-target effects, or subunit-specific. The longevity phenotype appeared specific to the gut, since no significant lifespan extension was observed upon induction of *dC160^{RNAi}* in the adult fly fat-body and only a modest, albeit significant extension resulted from neuronal induction (**Extended Data Fig. 4e and f**); fat-body and neurons being other two sites often associated with longevity¹³.

Worm gut is composed of only post-mitotic cells. In flies, like in mammals, the adult gut epithelium contains the mitotically active ISCs¹⁵. ISC homeostasis is important for longevity¹⁶ and the *TIGS* gut driver appears active in at least some ISCs (**Extended Data Fig. 5**), prompting us to further restrict *dC160^{RNAi}* induction to solely this cell type. ISC-specific *dC160^{RNAi}*, achieved with the *GS5961* driver, was sufficient to promote longevity (**Fig. 2c**, see **Extended Data Fig. 4b and g** for controls). In summary, Pol III activity in the gut limits survival in worms and flies, and in the fly, Pol III can drive ageing specifically from the gut stem cell compartment.

We assessed the consequences of Pol III inhibition in the fly gut. Pol III acts to generate precursor-tRNAs (pre-tRNAs) that are rapidly processed to mature tRNAs. Due to their short half-lives, pre-tRNA are suitable readouts of *in-vivo* Pol III activity. Profiling the levels of *pre-tRNA^{His}*, *pre-tRNA^{Ala}* and *pre-tRNA^{Leu}*, relative to the levels of *U3*, a small nucleolar RNA transcribed by Pol II¹⁷, revealed a moderate but significant reduction in Pol III activity upon gut-specific induction of *dC160^{RNAi}* (**Fig. 2d**). The three Pols can be directly coordinated for the generation of translation machinery¹⁸. Indeed, Pol III inhibition had knock-on effects on Pol I but not Pol II-generated transcripts, revealing a partial cross-talk (**Extended Data Fig. 6a and b**). Consistent with reduced Pol III activity, *dC160^{RNAi}* reduced protein synthesis in the gut (**Fig. 2e, Extended Data Fig. 6c**). These effects (reduction in pre-tRNAs or protein synthesis) were not observed after feeding RU486 to the driver-alone control (**Extended Data Fig. 6d - f**). The reduction in protein synthesis was not pathological: total protein content of the gut was unaltered; fecundity, a sensitive readout of a female's nutritional status, was unaffected; and the flies' weight, triacylglycerol and protein levels also remained unchanged (**Extended Data Fig. 6g - i**). Reduced protein synthesis can liberate protein-folding machinery from protein production and increase homeostatic capacity¹⁹. Indeed, inducing *dC160^{RNAi}* in the gut increased the resistance of adult flies to a proteostatic challenge with tunicamycin (**Fig. 2f, and Extended Data Fig. 6j** for *TIGS*-alone control). Hence, Pol III can fine-tune the rate of protein synthesis in the adult fly gut, without obvious detrimental outcomes, while increasing resistance to proteotoxic stress.

Having demonstrated the relevance of Pol III for ageing, we examined whether it acts downstream of TORC1 for lifespan using the fruit fly. Numerous observations in several organisms support the model where TORC1 localises on Pol III-transcribed

loci and promotes the phosphorylation of the components of Pol III transcriptional machinery to activate transcription, in part by inhibition of the Pol III repressor, Maf1⁵. Using chromatin immunoprecipitation (ChIP) with two independently generated antibodies against *Drosophila* TOR^{20,21}, we observed the kinase enriched on Pol III-target genes in the adult fly, relative to Pol II targets (**Fig. 3a; Extended Data Fig. 7a to d, and e** for mock ChIP). Inhibition of TORC1 by feeding flies rapamycin reduced the levels of pre-tRNAs in whole flies (**Fig. 3b**). Rapamycin also reduced pre-tRNA levels specifically in the gut relative to *U3* (**Fig 3c**). Since rapamycin results in re-scaling of the gut, evidenced by the reduction in the organ's total RNA content (**Extended Data Fig. 7f**), we also confirmed that the drug reduced pre-tRNA levels relative to total RNA (**Extended Data Fig. 7g**). Interestingly, rapamycin did not cause a decrease in 45S pre-rRNA in the gut (**Extended Data Fig. 7h and i**), suggesting a lack of sustained Pol I inhibition. Additionally, gut-specific over-expression of *Maf1* reduced the levels of pre-tRNAs and extended lifespan (**Fig 3d, Extended Data Fig. 7j**), confirming this Pol III repressor acts on Pol III in the adult gut. Our data are consistent with TORC1 driving systemic and gut-specific Pol III activity in the adult fruit fly.

To examine whether Pol III is downstream of TORC1 for lifespan, we combined adult-onset Pol III inhibition with rapamycin treatment. Rapamycin feeding or gut-specific *dC160^{RNAi}* resulted in the same magnitude of lifespan extension (**Fig. 3e**). The two treatments were not additive (see **Extended Data Fig. 8a** for summary and statistical analyses), consistent with their acting in the same longevity pathway. The same was observed with RNAi against *dC53* in the gut (**Extended Data Fig. 8b**), as well as when *dC160^{RNAi}* expression was restricted to the ISCs (**Fig. 3f**). Importantly, rapamycin feeding also inhibited the phosphorylation of TORC1 substrate, S6 kinase³

(S6K), in both the gut and the whole fly, and decreased fecundity, whilst gut-specific induction of *C160^{RNAi}* did not (**Fig. 3g and h, Extended Data Fig. 8c - f**). This confirms that Pol III inhibition does not impact TORC1 activity, neither locally nor systemically, and hence, Pol III acts down-stream of TORC1 in ageing (**Fig. 3i**).

TORC1 inhibition is known to ameliorate age-related pathology and functional decline of the gut²². We examined whether inhibition of Pol III was sufficient to block the dysplasia resulting from ISC mis-differentiation by assessing the characteristic, age-dependent increase in dividing, phospho-histone H3 positive (pH3+) cells¹⁶. Inducing *dC160^{RNAi}* in the fly gut or solely in the ISCs ameliorated this pathology (**Extended Data Fig. 9a, Fig. 4a and b**). The treatment was also sufficient to counteract the age-related loss of gut barrier function, decreasing the number of flies displaying extra-intestinal accumulation of a blue food dye ("smurf" phenotype²³, **Extended Data Fig. 9b, Fig. 4c**). Interestingly, we also found that *rpc-1* RNAi feeding reduced the severity of age-related loss of gut-barrier function in worms (**Extended Data Fig. 9c**). In *Drosophila*, gut health²⁴ and TORC1 inhibition²⁵ are specifically linked to female survival. Indeed, induction of *dC160^{RNAi}* in the gut had a sexually dimorphic effect on lifespan, as the effect on males, albeit significant, was reduced in magnitude relative to females (**Extended Data Fig. 9d**). Overall, our data show that gut/ISC-restricted inhibition of Pol III, which extends lifespan, is sufficient to ameliorate age-related impairments in gut health, which may be causative or correlate with this longevity.

Our study demonstrates that adult-onset decrease in the growth-promoting, anabolic function mediated by Pol III in the gut, and specifically in the stem cell compartment, is sufficient to recapitulate the longevity benefits of rapamycin treatment. Pol III activity is essential for growth⁶; its detrimental effects on ageing

suggest an antagonistic pleiotropy²⁶ where wild-type levels of Pol III activity are optimised for growth and reproductive fitness in early life but prove detrimental for later health. We reveal a fundamental role for Pol III in adult physiology, implicating wild-type Pol III activity in age-related stem cell dysfunction, declining gut health and organismal survival, downstream of nutrient signalling pathways. The longevity resulting from partial Pol III inhibition in adulthood likely stems from the reduced provision of protein synthetic machinery, however, differential regulation of tRNA genes or Pol III-mediated changes to chromatin organisation may also be involved, as has been suggested in other contexts². The strong structural and functional conservation of Pol III in eukaryotes suggests that studies of its influence on mammalian ageing are warranted and may lead to important therapies.

Acknowledgments

The authors thank S. Grewal, B. Ohlstein, L. Partridge and S. Pletcher for fly lines; C. Bouchoux and F. Uhlmann for yeast reagents; G. Juhasz and A. Teleman for antibodies; E. Bolukbasi and L. Partridge for FLAG-tagged dTor construct and S2 cells; M. Hill and D. Ivanov for help with RNA-Seq analysis; L. Conder, A. Garaeva, D. Mostapha, G. Phillips and P. van der Poel for technical assistance and M. Piper, J. Bähler and the IHA members for support, comments and critical reading of the manuscript. Reagents were obtained from Developmental Studies Hybridoma Bank, Vienna Drosophila Resource Centre, Bloomington Stock Center and the CGC, which is funded by NIH Office of Research Infrastructure Programs (P40 OD010440). This work was funded in part by Biotechnology and Biological Sciences Research Council grant BB/M029093/1, Royal Society grant RG140694 and Medical Research Council grant MR/L018802/1 to NA, and Royal Society grant RG140122 to JMAT. MH and VT

received funding from the European Union's Horizon 2020 research and innovation programme under the Marie Skłodowska-Curie grant agreement No 642738. DF is a recipient of the UCL Impact PhD studentship.

Author contributions

NA conceived the study; DF and NA made the yeast strains and performed chronological lifespans; VT performed and analysed yeast replicative lifespans under supervision of MH; MAT and JWMG performed and analysed worm experiments under supervision of JMAT; DF, AJD, IK and NA performed and analysed fly experiments under supervision of NA; DF, MAT, JMAT and NA wrote the manuscript with contributions from AJD.

Author information

Reprints and permissions information is available at www.nature.com/reprints.

The authors declare no competing financial interests.

Correspondence and requests for materials should be addressed to:

NA: n.alic@ucl.ac.uk (lead contact), JMAT: j.m.a.tullet@kent.ac.uk (co-corresponding author).

References

- 1 Roeder, R. G. & Rutter, W. J. Multiple forms of DNA-dependent RNA polymerase in eukaryotic organisms. *Nature* **224**, 234-237 (1969).
- 2 Arimbasseri, A. G. & Maraia, R. J. RNA Polymerase III Advances: Structural and tRNA Functional Views. *Trends in biochemical sciences* **41**, 546-559, doi:10.1016/j.tibs.2016.03.003 (2016).
- 3 Kennedy, B. K. & Lamming, D. W. The Mechanistic Target of Rapamycin: The Grand ConducTOR of Metabolism and Aging. *Cell Metab* **23**, 990-1003, doi:10.1016/j.cmet.2016.05.009 (2016).
- 4 Vannini, A. & Cramer, P. Conservation between the RNA polymerase I, II, and III transcription initiation machineries. *Molecular cell* **45**, 439-446, doi:S1097-2765(12)00089-5 [pii]10.1016/j.molcel.2012.01.023 (2012).
- 5 Moir, R. D. & Willis, I. M. Regulation of pol III transcription by nutrient and stress signaling pathways. *Bba-Gene Regul Mech* **1829**, 361-375, doi:10.1016/j.bbagr.2012.11.001 (2013).
- 6 Grewal, S. S. Why should cancer biologists care about tRNAs? tRNA synthesis, mRNA translation and the control of growth. *Bba-Gene Regul Mech* **1849**, 898-907, doi:10.1016/j.bbagr.2014.12.005 (2015).
- 7 Vellai, T. *et al.* Genetics: influence of TOR kinase on lifespan in *C. elegans*. *Nature* **426**, 620 (2003).
- 8 Powers, R. W., 3rd, Kaeberlein, M., Caldwell, S. D., Kennedy, B. K. & Fields, S. Extension of chronological life span in yeast by decreased TOR pathway signaling. *Genes Dev* **20**, 174-184, doi:20/2/174 [pii]10.1101/gad.1381406 (2006).
- 9 Harrison, D. E. *et al.* Rapamycin fed late in life extends lifespan in genetically heterogeneous mice. *Nature* **460**, 392-395 (2009).
- 10 Bitto, A. *et al.* Transient rapamycin treatment can increase lifespan and healthspan in middle-aged mice. *eLife* **5**, doi:10.7554/eLife.16351 (2016).
- 11 Nishimura, K., Fukagawa, T., Takisawa, H., Kakimoto, T. & Kanemaki, M. An auxin-based degron system for the rapid depletion of proteins in nonplant cells. *Nature methods* **6**, 917-922, doi:nmeth.1401 [pii]10.1038/nmeth.1401 (2009).
- 12 Libina, N., Berman, J. R. & Kenyon, C. Tissue-specific activities of *C. elegans* DAF-16 in the regulation of lifespan. *Cell* **115**, 489-502 (2003).

- 13 Piper, M. D., Selman, C., McElwee, J. J. & Partridge, L. Separating cause from effect: how does insulin/IGF signalling control lifespan in worms, flies and mice? *J Intern Med* **263**, 179-191 (2008).
- 14 Espelt, M. V., Estevez, A. Y., Yin, X. & Strange, K. Oscillatory Ca²⁺ signaling in the isolated *Caenorhabditis elegans* intestine: role of the inositol-1,4,5-trisphosphate receptor and phospholipases C beta and gamma. *The Journal of general physiology* **126**, 379-392, doi:10.1085/jgp.200509355 (2005).
- 15 Lemaitre, B. & Miguel-Aliaga, I. The digestive tract of *Drosophila melanogaster*. *Annual review of genetics* **47**, 377-404, doi:10.1146/annurev-genet-111212-133343 (2013).
- 16 Biteau, B. *et al.* Lifespan Extension by Preserving Proliferative Homeostasis in *Drosophila*. *PLoS genetics* **6**, doi:doi:10.1371/journal.pgen.1001159 (2010).
- 17 Dieci, G., Preti, M. & Montanini, B. Eukaryotic snoRNAs: a paradigm for gene expression flexibility. *Genomics* **94**, 83-88, doi:10.1016/j.ygeno.2009.05.002 (2009).
- 18 Laferte, A. *et al.* The transcriptional activity of RNA polymerase I is a key determinant for the level of all ribosome components. *Genes Dev* **20**, 2030-2040, doi:20/15/2030 [pii]10.1101/gad.386106 (2006).
- 19 Harding, H. P., Zhang, Y., Bertolotti, A., Zeng, H. & Ron, D. Perk is essential for translational regulation and cell survival during the unfolded protein response. *Molecular cell* **5**, 897-904 (2000).
- 20 Nagy, P. *et al.* Atg17/FIP200 localizes to perilyosomal Ref(2) P aggregates and promotes autophagy by activation of Atg1 in *Drosophila*. *Autophagy* **10**, 453-467, doi:10.4161/auto.27442 (2014).
- 21 Tsokanos, F. F. *et al.* eIF4A inactivates TORC1 in response to amino acid starvation. *The EMBO journal* **35**, 1058-1076, doi:10.15252/embj.201593118 (2016).
- 22 Fan, X. L. *et al.* Rapamycin preserves gut homeostasis during *Drosophila* aging. *Oncotarget* **6**, 35274-35283, doi:10.18632/oncotarget.5895 (2015).
- 23 Rera, M., Clark, R. I. & Walker, D. W. Intestinal barrier dysfunction links metabolic and inflammatory markers of aging to death in *Drosophila*. *Proc Natl Acad Sci U S A* **109**, 21528-21533, doi:1215849110 [pii]10.1073/pnas.1215849110 (2012).

- 24 Regan, J. C. *et al.* Sex difference in pathology of the ageing gut mediates the greater response of female lifespan to dietary restriction. *eLife* **5**, e10956, doi:10.7554/eLife.10956 (2016).
- 25 Bjedov, I. *et al.* Mechanisms of life span extension by rapamycin in the fruit fly *Drosophila melanogaster*. *Cell Metab* **11**, 35-46 (2010).
- 26 Williams, G. C. Pleiotropy, Natural-Selection, and the Evolution of Senescence. *Evolution* **11**, 398-411, doi:Doi 10.2307/2406060 (1957).

Additional references for Methods

- 27 Verduyn, C., Postma, E., Scheffers, W. A. & Van Dijken, J. P. Effect of benzoic acid on metabolic fluxes in yeasts: a continuous-culture study on the regulation of respiration and alcoholic fermentation. *Yeast* **8**, 501-517, doi:10.1002/yea.320080703 (1992).
- 28 Lee, S. S., Avalos Vizcarra, I., Huberts, D. H., Lee, L. P. & Heinemann, M. Whole lifespan microscopic observation of budding yeast aging through a microfluidic dissection platform. *Proc Natl Acad Sci U S A* **109**, 4916-4920, doi:10.1073/pnas.1113505109 (2012).
- 29 Huberts, D. H. *et al.* Construction and use of a microfluidic dissection platform for long-term imaging of cellular processes in budding yeast. *Nature protocols* **8**, 1019-1027, doi:10.1038/nprot.2013.060 (2013).
- 30 Papagiannakis, A., Jonge, J., Zhang, Z. & Heinemann, M. Quantitative characterization of the auxin-inducible degron: a guide for dynamic protein depletion in single yeast cells. *Scientific Reports in press* (2017).
- 31 Gelino, S. *et al.* Intestinal Autophagy Improves Healthspan and Longevity in *C. elegans* during Dietary Restriction. *PLoS genetics* **12**, e1006135, doi:10.1371/journal.pgen.1006135 (2016).
- 32 Poirier, L., Shane, A., Zheng, J. & Seroude, L. Characterization of the *Drosophila* gene-switch system in aging studies: a cautionary tale. *Aging Cell* **7**, 758-770 (2008).
- 33 Mathur, D., Bost, A., Driver, I. & Ohlstein, B. A transient niche regulates the specification of *Drosophila* intestinal stem cells. *Science* **327**, 210-213 (2010).
- 34 Giannakou, M. E. *et al.* Long-lived *Drosophila* with overexpressed dFOXO in adult fat body. *Science* **305**, 361 (2004).

- 35 Niccoli, T. *et al.* Increased Glucose Transport into Neurons Rescues Abeta Toxicity in *Drosophila*. *Current biology : CB* **26**, 2291-2300, doi:10.1016/j.cub.2016.07.017 (2016).
- 36 Rideout, E. J., Marshall, L. & Grewal, S. S. *Drosophila* RNA polymerase III repressor Maf1 controls body size and developmental timing by modulating tRNAiMet synthesis and systemic insulin signaling. *Proc Natl Acad Sci U S A* **109**, 1139-1144, doi:1113311109 [pii]10.1073/pnas.1113311109 (2012).
- 37 Bass, T. M. *et al.* Optimization of dietary restriction protocols in *Drosophila*. *J Gerontol A Biol Sci Med Sci* **62**, 1071-1081, doi:62/10/1071 [pii] (2007).
- 38 Alic, N., Hoddinott, M. P., Vinti, G. & Partridge, L. Lifespan extension by increased expression of the *Drosophila* homologue of the IGFBP7 tumour suppressor. *Aging Cell* **10**, 137-147 (2011).
- 39 Hoogewijs, D., Houthoofd, K., Matthijssens, F., Vandesompele, J. & Vanfleteren, J. R. Selection and validation of a set of reliable reference genes for quantitative sod gene expression analysis in *C. elegans*. *BMC molecular biology* **9**, 9, doi:10.1186/1471-2199-9-9 (2008).
- 40 Friendewey, D., Dingermann, T., Cooley, L. & Soll, D. Processing of Precursor Transfer-Rnas in *Drosophila* Processing of the 3' End Involves an Endonucleolytic Cleavage and Occurs after 5' End Maturation. *Journal of Biological Chemistry* **260**, 449-454 (1985).
- 41 Chan, P. P. & Lowe, T. M. GtRNAdb: a database of transfer RNA genes detected in genomic sequence. *Nucleic Acids Res* **37**, D93-D97, doi:10.1093/nar/gkn787 (2009).
- 42 Patro, R., Duggal, G., Love, M. I., Irizarry, R. A. & Kingsford, C. Salmon provides fast and bias-aware quantification of transcript expression. *Nature methods* **14**, 417-419, doi:10.1038/nmeth.4197 (2017).
- 43 Love, M. I., Huber, W. & Anders, S. Moderated estimation of fold change and dispersion for RNA-seq data with DESeq2. *Genome Biology* **15**, doi:Artn 55010.1186/S13059-014-0550-8 (2014).
- 44 Hahn, K. *et al.* PP2A regulatory subunit PP2A-B' counteracts S6K phosphorylation. *Cell Metab* **11**, 438-444, doi:10.1016/j.cmet.2010.03.015 (2010).

- 1 45 Schmidt, E. K., Clavarino, G., Ceppi, M. & Pierre, P. SUnSET, a nonradioactive
2 method to monitor protein synthesis. *Nature methods* **6**, 275-277,
3 doi:10.1038/NMETH.1314 (2009).
- 4 46 Alic, N. *et al.* Genome-wide dFOXO targets and topology of the transcriptomic
5 response to stress and insulin signalling. *Mol Syst Biol* **7**, 502 (2011).
- 6 47 Alic, N. *et al.* Interplay of dFOXO and two ETS-family transcription factors
7 determines lifespan in *Drosophila melanogaster*. *PLoS genetics* **10**, e1004619,
8 doi:10.1371/journal.pgen.1004619PGENETICS-D-14-00538 [pii] (2014).
- 9 48 O'Brien, L. E., Soliman, S. S., Li, X. & Bilder, D. Altered modes of stem cell
10 division drive adaptive intestinal growth. *Cell* **147**, 603-614, doi:S0092-
11 8674(11)01081-6 [pii]10.1016/j.cell.2011.08.048 (2011).

Figure Legends

Figure 1 Inhibition of Pol III extends lifespan.

Treatment of the *RPC160-AID-myc pADH-OsTir-myc* budding yeast strain with 0, 0.125 and 0.25 mM IAA: **a**, triggers degradation of C160-AID-myc and **b**, extends its chronological lifespan, measured as colony formation after normalisation for optical density and 10-fold serial dilution ([a] and [b] show a representative of two experimental trials). Feeding N2 worms with *E. coli* expressing the *rpc-1* RNAi construct from L4 stage: **c**, reduces the levels of *rpc-1* mRNA ($p < 10^{-4}$, two-tailed *t*-test) and **d**, extends their lifespan relative to vector alone at 20°C in presence of FUDR ($p = 0.03$, log-rank test, $n = 86$ control, 94 *rpc-1* RNAi animals; representative of three trials). Female flies heterozygous for the *dC53^{EY}* allele display: **e**, a reduction in *dC53* transcript ($p = 10^{-4}$, two-tailed *t*-test, 95% confidence intervals [CI] = 0.89-1.1 wt, 0.64-0.71 *dC53^{EY/+}*) and **f**, extended lifespan ($p = 6 \times 10^{-13}$, log-rank test, $n = 152$ control, 144 *dC53^{EY/+}* animals; single trial). Bar charts show mean \pm Standard Error of the Mean (SEM), with n = number of biologically independent samples indicated and overlay showing individual data points. For more detailed demography and summary of worm and fly lifespan trials see **Extended Data Fig. 2c and 4a**. For gel source data, see **Sup. Fig. 1**.

Figure 2 Gut-specific inhibition of Pol III extends lifespan, reduces protein synthesis and increases tolerance to proteostatic stress.

a, Activating RNAi against *rpc-1* specifically in the worm gut, using the VP303 strain, extends worm lifespan at 20°C in presence of FUDR ($p = 0.02$, log-rank test, $n = 90$ control, 67 *rpc-1* RNAi animals; representative of two trials). **b**, Feeding RU486 to *TIGS>dC160^{RNAi}* female fruit flies to induce *dC160^{RNAi}* in the gut alone extends their lifespan ($p = 6 \times 10^{-16}$, log-rank test, $n = 150$ -RU486, 157 +RU486 animals; representative of three trials). **c**, Feeding RU486 to *GS5961>dC160^{RNAi}* female fruit flies to induce *dC160^{RNAi}* in the ISCs alone extends their lifespan ($p = 2 \times 10^{-4}$, log-rank test, $n = 139$ -RU486, 142 +RU486 animals; representative of three trials). Inducing *dC160^{RNAi}* in the gut with RU486 feeding of *TIGS>dC160^{RNAi}* females leads to: **d**, reduction in pre-tRNAs (mean \pm SEM, $p = 0.04$, Multivariate Analysis of Variance [MANOVA], $n = 10$ biologically independent samples per -/+RU486 condition, CI = 0.91-1.1, 0.76-1.0, 0.90-1.1, 0.75-0.92, 0.88-1.1, 0.68-1.0 left to right); **e**, reduction in gut protein synthesis, as quantified by ex-vivo puromycin incorporation and western

blotting (representative of three biologically independent repeats; see **Extended Data Fig. 6c**); **f**, improved survival in response to tunicomycin challenge ($p=3\times 10^{-15}$, *log-rank test*, $n=185$ animals per condition; representative of two trials). For more detailed demography and summary of lifespan trials see **Extended Data Fig. 2c** and **4a**. For gel source data, see **Sup. Fig. 1**.

Figure 3 Pol III acts downstream of TORC1 for lifespan.

a, Relative enrichment of Pol III-transcribed genes is higher than that of Pol II-transcribed genes after ChIP against TOR ($p<10^{-4}$, *Linear Model [LM]* with an *a priori* contrast, $n=3$ biologically independent samples). Rapamycin feeding causes a decrease in pre-tRNAs relative to U3 in: **b**, whole female flies ($p=0.01$, *MANOVA*, CI= 0.76-1.2, 0.58-0.79, 0.75-1.3, 0.49-0.79, 0.70-1.3, 0.48-0.78 left to right); **c**, their guts ($p=0.01$, *MANOVA*, CI= 0.98-1.1, 0.90-1.0, 0.87-1.1, 0.74-0.99, 0.90-1.1, 0.77-0.97 left to right). **d**, Induction of *Maf1* in the guts of *TIGS>HA-Maf1* females by RU486 feeding reduces the levels of pre-tRNAs relative to U3 ($p=4\times 10^{-3}$, *MANOVA*, CI= 0.87-1.1, 0.74-1.0, 0.90-1.1, 0.82-1.0, 0.76-1.2, 0.53-1.0 left to right). **e**, Induction of *dC160^{RNAi}* in the adult guts by RU486 feeding of *TIGS>dC160^{RNAi}* females and rapamycin feeding both extend lifespan and are not additive (effect of rapamycin $p=2\times 10^{-14}$, effect of RU486 $p<2\times 10^{-16}$, interaction $p=7\times 10^{-9}$, *Cox Proportional Hazards [CPH]*, $n=135$ control, 144 +RU486, 141 +rapamycin and 146 +RU486 and rapamycin animals; single trial). **f**, Induction of *dC160^{RNAi}* in the ISCs by RU486 in *GS5961>dC160^{RNAi}* females and rapamycin both extend lifespan and are not additive (effect of rapamycin $p=8\times 10^{-14}$, effect of RU486 $p=2\times 10^{-5}$, interaction $p=3\times 10^{-7}$, *CPH*, $n=113$ control, 130 +RU486, 145 +rapamycin and 144 +RU486 and rapamycin animals; single trial). Rapamycin but not *dC160^{RNAi}* induction in the gut by RU486 feeding of *TIGS>dC160^{RNAi}* females leads to: **g**, reduction in S6K phosphorylation in the gut or the whole fly (representative of four biologically independent repeats; see **Extended Data Fig. 6c-f**); **h**, reduction in egg laying (effect of rapamycin $p<10^{-4}$, RU486 $p=0.87$ and interaction $p=0.96$, *LM*). **i**, Model of the relationship between TORC1, Pol III and lifespan. Bar charts show mean \pm SEM, with n = number of biologically independent samples indicated and overlay showing individual data points. For more detailed demography, statistics and summary of lifespan trials see **Extended Data Fig. 8a**. For gel source data see **Sup. Fig. 1**

Figure 4 Stem cell-restricted Pol III inhibition improves age-related dysplasia and gut barrier function.

dC160^{RNAi} induction in the ISCs of adult *GS5961>dC160^{RNAi}* females by RU486 feeding suppresses age-related accumulation of pH3 positive cells: **a**, images of pH3 staining in the posterior mid-gut at 70 d of age (white bar = 100 μ m, white “>” marks pH3+ cells, representative of seven -RU486 and nine +RU486 animals); **b**, the number of pH3+ cells per gut (effect of age $p < 10^{-4}$, RU486 $p = 2 \times 10^{-3}$, interaction $p = 2 \times 10^{-3}$, *LM*, young: 7-9 d, old: 56-70 d, CI= 2.6-8.6, 1.8-9.4, 14-36, 6.0-14 left to right). **c**, *dC160^{RNAi}* induction in the ISCs of adult *GS5961>dC160^{RNAi}* females by RU486 feeding reduces the age-related increase in the number of flies with a leaky gut (effect of age $p < 10^{-4}$, RU486 $p = 0.09$, interaction $p = 0.01$, *Ordinal Logistic Regression*, young: 21 d, old: 58 d, CI= 0.19-0.28, 1.5-1.8, 18-19, 14-15 % smurf left to right). Bar charts show mean \pm SEM, with n= number of biologically independent animals indicated and overlay showing individual data points.

Methods

Yeast stocks, chronological lifespans and microfluidics assessment

pMK43-based cassette was integrated into w303 *MATa leu2-3,112 trp1-1 can1-100 ura3-1 pADH-OsTir-9Myc::ADE2::ade2-1 his3-11,15* to produce *RPC160* or *RPB220* C-terminal AID fusions as described¹¹, confirmed by PCR and absence of growth in presence of 2.5 mM IAA.

Primers for strain construction:

<i>C160 Fw</i>	<i>TGTCTATTTGAAAGTCTCTCAAATGAGGCAGCTTTAAAAGCGAACCGTACGCTGCAGGTCGAC</i>
<i>C160 Rv</i>	<i>AGAAAAATAATACAAATGCTATAAAAAAGTTTAAAAACGACTACTATCGATGAATTCGAGCTCG</i>
<i>B220 Fw</i>	<i>CCAAAGCAAGACGAACAAAAGCATAATGAAAATGAAAATTCCAGACGTACGCTGCAGGTCGAC</i>
<i>B220 Rv</i>	<i>ATATATAATGTAATAACGTCAAATACGTAAGGATGATATACTATAATCGATGAATTCGAGCTCG</i>

Primers for verification:

<i>C160 Fw</i>	<i>TTGGGTCAAACGATGTCTG</i>
----------------	----------------------------

B220 Fw *CGCCTTCATACTCTCCAAC*
C160/B220 Rv *TGCCCATCATGGTACCTG*

For chronological lifespans, the strains were grown to exponential phase (OD₆₀₀~0.4) in Synthetic Complete medium (2% glucose, 0.5% ammonium sulphate, 0.17% yeast nitrogen base, 0.001% adenine, uracil, tryptophan, histidine, arginine, methionine, 0.0025% phenylalanine, 0.003% tyrosine, lysine, 0.004% isoleucine, 0.005% glutamate, aspartate, 0.0075% valine, 0.01% threonine, 0.02% serine and leucine [w/v]), the culture split and treated with IAA in acetone or acetone alone (0.1%, day 0) and kept with aeration and shaking at 30°C. Cells were harvested for protein extraction after 30 min. Cultures essentially reached stationary phase after 24h. The viability was measured on the indicated days by plating 5 µl of 10-fold serial dilutions starting from initial concentration corresponding to OD₆₀₀=0.5 on YEPD plates and growth for 2 d at 30°C.

For replicative lifespan, cells from single colonies were inoculated in 10 mL of minimal medium²⁷ with 1% glucose, 0.02% leucine and 0.001% tryptophan, arginine, histidine and uracil (w/v) and pH 5 maintained with K-Phthalate-KOH buffer. The 10 mL cultures were cultivated overnight in 100 mL shake flasks at 30°C and 300 rpm. Still exponential, they were diluted next morning to OD₆₀₀ of 0.005-0.01 and cultivated for several hours to OD₆₀₀ of 0.045-0.09 when they were loaded into the microfluidics device as described^{28,29}. The growth medium was aerated in advance by shaking for at least two hours. Trapped in the device, the cells were constantly provided with fresh medium containing the synthetic auxin hormone 1-naphthaleneacetic acid (NAA) at the concentrations of 0.0005, 0.001, 0.005 or 0.01 mM; the control did not contain NAA. These concentrations of the hormone span through the dynamic range of the auxin-based degron system where the degree of protein depletion can be efficiently

modulated in the set-up used³⁰. Temperature of 30°C was maintained throughout the experiment.

Microscopic imaging in the bright field channel was performed for up to 5 days with the time interval of 5 minutes, using a Nikon Ti-E inverted microscope equipped with a 40x Nikon Super Fluor Apochromat objective, and halogen lamp with additional UV-blocking filter. For each cell, the time points of (1) the budding events, (2) the eventual cell losses due to wash away, or (3) cell death were recorded by visual inspection of the movies with the help of ImageJ and a custom written macro. For assessment of cell division times, the first six cell cycles of each cell were used.

Worm husbandry, lifespans and gut integrity assay.

Prior to experiments animals were maintained at 20°C and grown for at least three generations with ample OP50 *Escherichia coli* food to assure full viability. The *rpc-1* RNAi clone, gene code C42D4.8, was obtained from the Ahringer library. Lifespan assays were performed on HT115 *E. coli* expressing either the *rpc-1* RNAi plasmid or pL4440 empty vector control. Experiments were carried out at both 20°C and 25°C. Worms were scored as dead or alive at intervals and worms that crawled off the plate or died from explosion or bagging phenotypes were censored. *rpc-1* RNAi treatment from L4 stage increased the incidence of a vulval explosion phenotype (noted in **Extended Data Fig. 2c**). However, we found that at 25°C this phenotype was greatly reduced (**Extended Data Fig. 2c**). For gut-restricted RNAi, the VP303 strain was used¹⁴. The “smurf” assay for gut integrity was carried out essentially as described³¹. Worms were aged from the L4 stage at 25°C and on the appropriate day soaked in blue dye for 3 hours. The dye was removed by allowing the worms to crawl around on a bacterial lawn for 30 minutes prior to microscopy analysis. Individual

worms were scored from 0-4 for their degree of “smurfness” with 0 being no blue beyond the gut barrier and 4 being completely blue.

Fly husbandry, lifespan, tunicamycin survival, smurf and fecundity assays

The outbred, wild-type stock was collected in 1970 in Dahomey (now Benin) and has been kept in population cages to maintain lifespan and fecundity at levels similar to wild-caught flies. *w*¹¹¹⁸ mutation was backcrossed into the stock and *Wolbachia* cleared by tetracycline treatment. *TIGS*³² (a.k.a. *TIGS-2*), *GS5961*³³, *S₁106*³⁴, *elavGS*³⁵, *UAS-HA-Maf1*³⁶, *UAS-dC160*^{RNAi} and *UAS-dC53*^{RNAi} (v30512 and v103810 from Vienna Drosophila Resource Centre), and *dC53*^{EY22749} (*CG5147*^{EY22749} from Bloomington Stock Centre) were all backcrossed at least 6 times into the *w*¹¹¹⁸ Dahomey background.

Stocks were maintained and experiments conducted at 25°C on a 12L:12D cycle at 60% humidity, on SYA food³⁷ containing 10% brewer’s yeast, 5% sucrose, and 1.5% agar (all w/v; with propionic acid and Nipagin as preservatives). RU486 (Sigma) and Rapamycin (LC Laboratories, both dissolved in ethanol) were added to 200µM final concentration as required. Tunicamycin (Cell Signaling, DMSO stock) was used in food with only sugar and agar at concentration of 10mg/l. For control treatments, equivalent volumes of the vehicle alone were added.

Flies were reared at standardised larval density and adults collected over 12 h, allowed to mate for 48 h and sorted into experimental vials at a density of 15 flies per vial (10 flies per vial for RNA extractions). For lifespan experiments, flies were transferred to fresh vials and their survival scored three times a week. Flies were transferred onto food containing tunicamycin on day 9 and survival scored once or twice daily. For smurf assays, at the indicated age the flies were placed on SYA food

containing 2.5% (w/v) blue dye (FD&C blue dye no. 1, Fastcolors) for 48 h and scored as full smurfs if completely blue or partial smurfs if the dye had leaked out of the gut but not reached the head. Eggs layed over ~24h were counted on day 10. Other phenotypic tests were performed essentially as described³⁸.

RNA extraction, qPCR and RNA-Seq

Synchronised populations of worms were placed on control or *rpc-1* RNAi at the L4 stage, grown at 20°C and harvested after 4 days. Ten whole adult flies, or ten dissected mid-guts, were harvested on day 7-9. Total RNA was isolated using TRIZOL (Invitrogen). RNA isolation was quantitative – the amount obtained was proportional to the starting amount. RNA was converted to cDNA using random hexamers and Superscript II (Invitrogen). Quantitative PCR was performed using Power SYBR Green PCR Master Mix (ABI), with the relative standard curve method. For worms, *rpc-1* transcript levels were normalised to the geometric mean of three stably expressed reference genes *cdc-42*, *pmp-3* and *Y45F10D.4* as described³⁹. For flies, primers specific for pre-tRNAs were designed based on previous biochemical characterisation⁴⁰ or predicted intronic sequences⁴¹.

Primer sequences:

Flies:

Gene of Interest	Forward Primer	Reverse Primer
<i>dC53</i> (<i>CG5147</i>)	GGGTGACCCAGAGTCCCT	GGCGAGCTCAGCGAAGAG
<i>pre-rRNA ITS</i>	<i>TTAGTGTGGGGCTTGGCAACCT</i>	<i>CGCCGTTGTTGTAAGTACTCGCC</i>
<i>pre-rRNA ETS</i>	<i>GTTGCCGACCTCGCATTGTTTCG</i>	<i>CGGAGCCAAGTCCCGTGTTCAA</i>
<i>pre-tRNA^{HIS}</i>	CGTGATCGTCTAGTGGTTAG	CCCAACTCCGTGACAATG
<i>pre-tRNA^{ALA}</i>	CGCACGGTACTTATAATCAG	CCAGGTGAGGCTCGAACTC
<i>pre-tRNA^{LEU}</i>	GCGCCAGACTCAAGATTG	TGTCAGAAGTGGGATTTCG

1	<i>Tub</i>	TGGGCCCCGTCTGGACCACAA	TCGCCGTCACCGGAGTCCAT
2	<i>U3</i>	CACACTAGCTGAAAGCCAAG	CGAAGCCCTGCGTCCCGAAC
3			
4	Worms:		
5	Gene of Interest	Forward Primer	Reverse Primer
6	<i>rpc-1</i>	ACGATGGATCACTTGTTTGAAGC	GTTCCGACAGTCATTGGGGT
7	<i>cdc-42</i>	CTGCTGGACAGGAAGATTACG	CTCGGACATTCTCGAATGAAG
8	<i>pmp-3</i>	GTTCCCGTGTTTCATCACTCAT	ACACCGTCGAGAAGCTGTAGA
9	<i>Y45F10D.4</i>	GTCGCTTCAAATCAGTTCAGC	GTTCTTGTC AAGTGATCCGACA

For RNA-Seq, RNA was further cleaned up with Qiagen RNeasy (Qiagen), ribo-depleted (Ribo-Zero Gold; Illumina) and sequenced on the Illumina platform at Glasgow Polyomics (75 bp, pair-end reads). Transcript abundance was estimated with Salmon⁴² (<https://combine-lab.github.io/salmon/>) in quazi-mapping mode onto all *Drosophila* cDNA sequences (BDGP6), imported with tximport (<https://bioconductor.org/packages/release/bioc/html/tximport.html>) into R (<https://www.r-project.org/>) and differential expression determined with DESeq2 (<https://bioconductor.org/packages/release/bioc/html/DESeq2.html>) using dissection batch as covariate at 10% false discovery rate⁴³.

Western blots, immunoprecipitation (IP), S2 dsRNA treatment, translation assays and ChIP

Proteins were extracted from yeast (10 ml culture), S2 cells (0.1-2 ml culture; S2 cells were obtained from L. Partridge), 10 flies or ten dissected mid-guts with trichloroacetic acid, washed and re-suspended in SDS-PAGE loading buffer, separated by SDS-PAGE and transferred to nitrocellulose. Western blots were performed with anti-puromycin 12D10 antibody (Millipore), anti-Actin (Abcam, ab1801

or ab8224), anti-Myc (Sigma), anti-FLAG (Sigma), anti-phospho-T398-S6K (Cell Signaling, 9209), anti-S6K antibody⁴⁴ or anti-TOR antibody²⁰.

IPs were performed on ~2mg of total protein extracted from 2-5 ml of S2 cell culture (transfected with pAFW-dTOR, treated with dsRNA or untreated) into 50mM HEPES-KOH pH 8, 100 mM KCl, 5 mM EDTA, 10% glycerol, 0.5% NP-40 and protease inhibitors with 0.5 µl of anti-dTOR serum²⁰, washed five times with the same buffer and eluted into SDS-PAGE sample buffer. dsRNA against *dTOR* corresponds to fragment 3694-4208 bp of the *dTOR* open reading frame (this is DRSC02811 from DRSC/TRiP) and was generated with Megascript RNAi Kit (Thermo Fisher Scientific).

Relative translation rates were determined with the SUNSET assay⁴⁵: 10 mid-guts of 7 day old flies per sample were dissected in ice-cold PBS and kept in 200 µl of ice-cold Schneider's medium followed by incubation in 1 ml of Schneider's medium with 10 µg/ml puromycin for 30 min at 25°C. 333 µl of 50 % trichloroacetic acid were added to stop the reaction. Level of puromycin incorporation was determined by western blots.

ChIP was performed as described⁴⁶ on chromatin prepared from 7-day old, wild-type females using either the anti-TOR antibody raised against a recombinant TOR protein fragment²⁰, or anti-TOR raised against a peptide²¹. The mock control included no antibody. Enrichment after IP was measured relative to input with qPCR. Primers for 5' and 3' end of *aop* and the P2 *InR* promoter have been described^{46,47}.

Further primers used:

Gene of Interest	Forward Primer	Reverse Primer
5S rRNA	GCCAACGACCATAACCACGCTG	AGTACTAACCGCGCCCGACG
tRNA ^{MET}	CGCAGTTGGCAGCGCGTAAG	CCCCGGGTGAGGCTCGAACT

pH3, Prospero and anti-HRP staining

Guts were dissected at indicated ages in ice-cold PBS and immediately fixed in 4% formaldehyde for 30 minutes. The staining was performed essentially as described³⁸ with anti-phospho-H3 antibody (Cell Signaling, 9701), anti-Prospero (Developmental Studies Hybridoma Bank) or anti-HRP⁴⁸. Guts were mounted in mounting medium with DAPI (Vectastain). pH3 positive cells per midgut were counted on a fluorescence microscope. Representative images were acquired with the Zeiss LSM700 confocal microscope.

Statistical Analysis

Fly and worm: Survival assays were analysed with *log-rank* test in Excel (Microsoft) or JMP (SAS), or with *CPH* in R using the *survival* package (<https://cran.r-project.org/web/packages/survival/index.html>). All other tests were performed in JMP. Data obtained from dissections, ChIP or westerns were scaled to dissection/chromatin/replicate batch, except for pH3 counts, to account for batching effects. *MANOVA* was used to test for overall effect of RU486 or rapamycin feeding. For ChIP analysis, “gene” was used as covariate in a *LM* with an *a priori* contrast comparing Pol III- to Pol II-transcribed genes. All regression models had a fully factorial design.

Yeast microfluidics platform: The data, including the number of buds produced by each cell and its final event (death or washout), were used for Kaplan-Meier estimation of survival curves with the Lifelines module (Davidson-Pilon, C., Lifelines, (2016), Github repository, <https://github.com/CamDavidsonPilon/lifelines>) in Python. Plotting and statistical analysis were done in Python.

Code Availability statement

1 A custom designed code was used to analyse the yeast replicative lifespan
2 data and will be made available upon reasonable request.

3
4 **Data Availability statement**

5 The data that support the findings of this study are available within the paper
6 and its supplementary information files, including source data for figures, or are
7 available from the corresponding author upon reasonable request. RNA-Seq data
8 have been deposited in ArrayExpress: accession code E-MTAB-5252.

Extended Data Legends

Extended Data Figure 1. Inhibition of Pol III in yeast.

a, The growth of strains carrying *pADH-OsTir* with *RPC160-AID*, *RPB220-AID* or the control lacking any AID fusion in the presence or absence of 2.5 mM IAA (single trial). **b**, Chronological lifespans of the control and *RPB220-AID* strains treated with 0, 0.125 and 0.25 mM IAA. Top panels show a representative of two experiments, performed in parallel with *RPC160-AID* shown in **Fig. 1b**. The bottom panels show a single experiment; the improved survival of *RPB220-AID* was also observed at a higher IAA concentration in a second experiment. **c**, Yeast replicative lifespan (top panels) is not altered by 1-naphthaleneacetic acid (NAA; analogue of IAA) while cell cycle duration (bottom panels) is. Both were assessed in the *pADH-OsTir RPC160-AID* strain on a microfluidics dissection platform. The concentrations of NAA span the dynamic range where the degree of protein depletion can be efficiently modulated in this set-up³⁰. The same control data are shown in each panel for comparison. For each NAA concentration one experiment was performed. For replicative lifespans, 95% CIs are indicated by shading, or in brackets for median lifespan, together with *log-rank* p value. One-sided *Mann-Whitney U* test was used to test for significant differences in cell cycle duration. No adjustments were made for multiple comparisons. Dashed lines on bottom panels represent medians.

Extended data Figure 2. Inhibition of Pol III extends worm lifespan.

a, Lifespan is extended by feeding N2 worms with *rpc-1* RNAi at 20°C in absence of FUDR ($p < 10^{-3}$ *log-rank* test, $n = 100$ control and *rpc-1* RNAi treated animals). **b**, It is also extended at 25°C in presence of FUDR ($p = 9 \times 10^{-3}$, *log-rank* test, $n = 60$ control, 77 *rpc-1* RNAi animals). **c**, Summary of each worm lifespan experiment performed including the representative trials presented in the figures. *Log-rank* test p value is reported. The total number of animals in the trial = dead + censored. In general, fewer worms were censored in control vs *rpc-1* RNAi conditions (average of N2 at 25°C 25% vs 38%; average of N2 at 20°C 53% vs 73%; average of VP303 at 25°C 3% vs 4% and average of VP303 at 20°C 37% vs 54%) which is likely to be due to an increased number of gut explosions in the *rpc-1* RNAi treated worms. On average 84.9% of control and 85.6% of *rpc-1* RNAi-treated censored events occurred before the 25th percentile of the survival curve. Overall, increasing the temperature to 25°C reduced

censoring without altering our findings. **d**, Lifespan is extended when the RNAi against *rpc-1* is restricted to the gut using VP303 strain, at 25°C in presence of FUDR ($p=9 \times 10^{-3}$, *log-rank test*, $n= 84$ control, 103 *rpc-1* RNAi treated animals). In (a), (b) and (d), a representative of two trials is shown.

Extended data Figure 3. Genes corresponding to unique Pol III subunits in *Drosophila*.

The genes encoding the unique Pol III subunits were identified in fruit flies based on their homology to the yeast genes (BLAST, followed by reverse BLAST), or to the human orthologue.

Extended Data Figure 4. Inhibition of Pol III extends fly lifespan.

a, Summary of each fly lifespan experiment performed including the representative trials presented in the figures but excluding the ones with rapamycin (see **Extended Data Fig. 8a**). Experiments were performed on females unless otherwise noted. The total number of animals in the trial = dead + censored. *Log-rank test* p value is reported. RU486 feeding does not have an effect on the lifespans of: **b**, *UAS-dC160^{RNAi}* alone ($p=0.28$, *log-rank test*, $n= 142$ -RU486, 146 +RU486 animals); or **c**, *TIGS* alone controls ($p=0.41$, *log-rank test*, $n= 141$ -RU486, 145 +RU486 animals). **d**, Inducing *dC53^{RNAi}* in the gut of *TIGS>dC53^{RNAi}* females by RU486 extends their lifespan ($p=3 \times 10^{-6}$, *log-rank test*, $n= 143$ -RU486, 139 +RU486 animals). **e**, Inducing *dC160^{RNAi}* predominantly in the fat body of *S₁106>dC160^{RNAi}* females by RU486 has no effect on their lifespan ($p=0.21$, *log-rank test*, $n= 158$ -RU486, 155 +RU486 animals). **f**, Inducing *dC160^{RNAi}* in neurons of *elavGS>dC160^{RNAi}* females by RU486 has a modest effect on their lifespan ($p=0.03$, *log-rank test*, $n= 148$ -RU486, 155 +RU486 animals). **g**, RU486 feeding does not have an effect on the lifespan of the *GS5961* alone control ($p=0.88$, *log-rank test*, $n= 89$ -RU486, 91 +RU486 animals). In (b) to (g) the single trial performed is shown.

Extended Data Figure 5. *TIGS* is active in ISCs.

Images from the posterior region of the midgut showing GFP expression driven by *TIGS* in the presence of RU486 and stained with: **a**, anti-Prospero; **b**, anti-HRP. GFP expression can be observed in cells with small nuclei that are Prospero-negative in (a) and those that stain with anti-HRP in (b). Examples of both types are indicated with a

white “>” on the merged images. GFP-positive cells can be observed whose morphology and staining pattern correspond closely to that of the ISCs (small nucleus, small cell size, Prospero-negative, anti-HRP-positive [see ref. ⁴⁸ regarding anti-HRP]). *TIGS* has a complex expression pattern, showing variation between neighbouring cells of the same type and between gut regions. *TIGS* appears active in at least some ISCs. Images are representative of two animals.

Extended Data Figure 6. Effects of *dC160*^{RNAi} induction in *Drosophila* adult gut.

Induction of *dC160*^{RNAi} in the guts of *TIGS>dC160*^{RNAi} females results in: **a**, decreased levels of 45S pre-rRNA ($p=4\times 10^{-3}$, MANOVA, CI= 0.95-1.1, 0.85-1.0, 0.95-1.1, 0.81-0.92 left to right; EST = 5' external transcribed spacer, IST = internal transcribed spacer), indicating a reduction in Pol I activity as a result of Pol III – Pol I crosstalk; **b**, unaltered levels of mRNAs encoding ribosomal proteins (RNA-Seq data, no significant differences at 10% false discovery rate, DESeq2, n= 3 biologically independent samples), indicating no crosstalk between Pol III and Pol II; **c**, decreased protein synthesis (two further biological repeats and quantification related to **Fig. 2e**; $p=4\times 10^{-3}$, two-sided *t*-test, n=3 biologically independent samples, CI= 0.65-1.4 -RU486, -0.033-0.68 +RU486). RU486 feeding of *TIGS*-alone control females does not result in a significant decrease in: **d**, levels of pre-tRNAs ($p=1\times 10^{-4}$, MANOVA, CI= 0.96-1.0, 1.1-1.2, 0.93-1.1, 1.1-1.2, 0.91-1.1, 1.2-1.3 left to right); **e**, levels of 45S pre-rRNA ($p=2\times 10^{-4}$, MANOVA, CI= 0.94-1.1, 1.1-1.3, 0.94-1.1, 1.1-1.2 left to right); **f**, protein synthesis ($p=0.74$, two-sided *t*-test, n=3 biologically independent samples). Induction of *dC160*^{RNAi} in the guts of *TIGS>dC160*^{RNAi} females does not result in significant changes to: **g**, total gut protein content ($p=0.43$, two-sided *t*-test); **h**, female fecundity ($p=0.51$, two-sided *t*-test); **i**, whole-fly body weight, triacylglycerol or protein content ($p=0.58$, 0.40, 0.16 respectively, two-sided *t*-test). **j**, RU486 feeding of *TIGS*-alone control females does not result in increased resistance to tunicamycin ($p=0.89$, log-rank test, n= 149 -RU486, 153 +RU486 animals; single trial). Bar charts show mean \pm SEM, with n= number of biologically independent samples indicated and overlay showing individual data points. For gel source data see **Sup. Fig. 1**.

Extended Data Figure 7. Regulation of Pol III activity by TORC1 in *Drosophila*.

a, The antibody raised against a recombinant fragment of *Drosophila* TOR protein ²⁰ and used for ChIP (**Fig. 3a**) recognises a single band of the expected size on western

blots of S2 cell extracts. **b**, The same antibody can immunoprecipitate (IP) dTOR from S2 cells expressing the endogenous and FLAG-tagged dTOR. **c**, It can also IP endogenous dTOR and the intensity of this band is reduced upon treatment of S2 cells with dsRNA against *dTOR*. For (a) to (c), a single experiment was performed; the ability of the *dTOR* RNAi to reduce the intensity of the band was confirmed in an independent experiment. **d**, Relative enrichment of Pol III-transcribed genes is higher than that of Pol II-transcribed genes after ChIP using a second antibody against *Drosophila* TOR (raised against a peptide²¹, $p=2\times 10^{-4}$; *LM* with an *a priori* contrast, $n=3$ biologically independent samples, CI= 1.6-2.6, 0.81-2.3, 1.1-2.7, 0.77-2.8, -0.24-2.5, -0.065-2.0, 0.13-1.7 left to right). **e**, No enrichment for Pol III-transcribed genes over Pol II-transcribed genes is observed after mock ChIP with no antibody ($p=0.09$, *LM* with an *a priori* contrast, $n=3$ biologically independent samples). **f**, Rapamycin feeding results in a decrease in total RNA content of the adult gut ($p<10^{-4}$, two-sided *t-test*). **g**, Rapamycin feeding results in reduction of pre-tRNAs relative to total RNA in the fly gut ($p=10^{-4}$, *MANOVA*). Rapamycin feeding does not result in a reduction of pre-rRNA in the fly gut relative to: **h**, *U3* ($p<10^{-4}$, *MANOVA*); **i**, total RNA ($p=0.57$, *MANOVA*). **j**, Feeding RU486 to *TIGS>HA-Maf1* female fruit flies to induce *HA-Maf1* in the gut alone extends their lifespan ($p=0.006$, *log-rank test*, $n=153$ -RU486, 146 +RU486 animals; single trial). Bar charts show mean \pm SEM, with n = number of biologically independent samples indicated and overlay showing individual data points. For gel source data see **Sup. Fig. 1**.

Extended Data Figure 8. Relationship between TORC1 and Pol III.

a, Summary of fly lifespans examining the epistasis between Pol III and TORC1 inhibition (top), including the CPH analyses results (bottom). In the summary (top), *log-rank test* p value, relative to -RU486 -rapamycin control, is reported and the total number of animals in the trial = dead + censored. **b**, Induction of *dC53^{RNAi}* in the adult guts by RU486 feeding of *TIGS>dC53^{RNAi}* females and rapamycin feeding both extend lifespan and are not additive (for statistical analysis see [a]; $n=135$ control, 135 +RU486, 120 +rapamycin and 137 +RU486 and rapamycin animals; single trial). **c - f**, Rapamycin but not induction of *dC160^{RNAi}* in the guts of *TIGS>dC160^{RNAi}* females by RU486 reduces the phosphorylation of S6K in the gut (effect of rapamycin $p=3\times 10^{-4}$, RU486 $p=0.77$ and interaction $p=0.55$, *LM*, CI= 0.51-1.5, 1.0-1.2, 0.33-0.73, 0.08-0.91 left to right) and whole flies (effect of rapamycin $p<10^{-4}$, RU486 $p=0.10$ and interaction

p=0.16, *LM*, CI=0.77-1.2, 0.60-1.0, 0.016-0.19, 0.019-0.15 left to right). Further biological repeats related to **Fig. 3g** are presented in (c) for the gut and in (d) for the whole fly. These are quantified in (e) and (f) respectively. In (c) to (f), data from four biologically independent samples are shown. For gel source data see **Sup. Fig. 1**.

Extended Data Figure 9. Inhibition of Pol III in the gut preserves organ health.

a, *dC160^{RNAi}* induction in the gut of adult *TIGS>dC160^{RNAi}* females by RU486 feeding suppresses accumulation of pH3 positive cells in old flies ($p=1 \times 10^{-3}$, 2-tailed *t*-test, CI=58-110 -RU486, 10-46 +RU486). **b**, *dC160^{RNAi}* induction in the gut of adult *TIGS>dC160^{RNAi}* females by RU486 feeding suppresses loss of gut barrier function (number of “smurfs”) in old flies ($p=5 \times 10^{-4}$, χ^2 -test, CI=16-26 -RU486, 8.7-16 +RU486 % smurf). **c**, *rpc-1* RNAi suppresses the severity of the age-related loss of gut barrier function in worms (effect of age $p < 10^{-4}$, *rpc-1* RNAi $p=0.51$, interaction $p=0.01$, *Ordinal Logistic Regression*, CI=5.0-31, 16-50, 24-48, 25-51, 53-78, 34-66 % smurf grades 3 and 4). Age-related loss of gut barrier function has been previously described for worms³¹. **d**, *dC160^{RNAi}* induction in the gut of adult *TIGS>dC160^{RNAi}* males by RU486 feeding results in a small but significant extension of lifespan ($p=0.03$, *log-rank-test*, $n=141$ -RU486, 139 +RU486 animals; single trial). Bar charts show mean \pm SEM with n = number of animals indicated and overlay showing individual data points.

Fig. 1

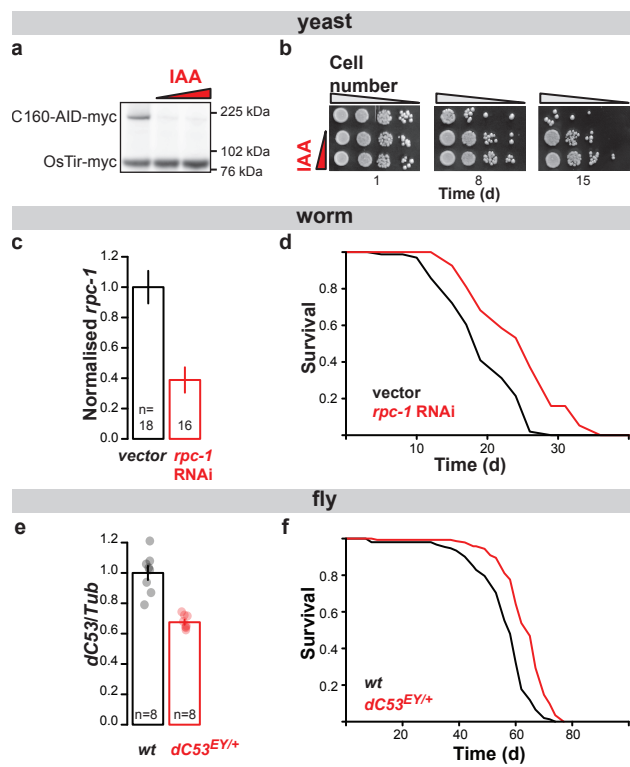


Fig. 2

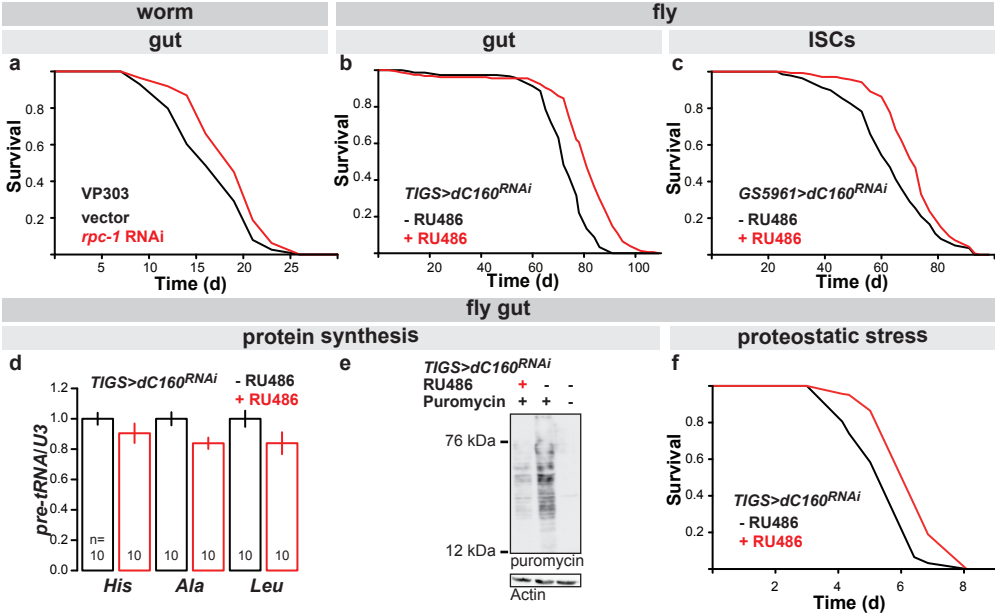


Fig. 3

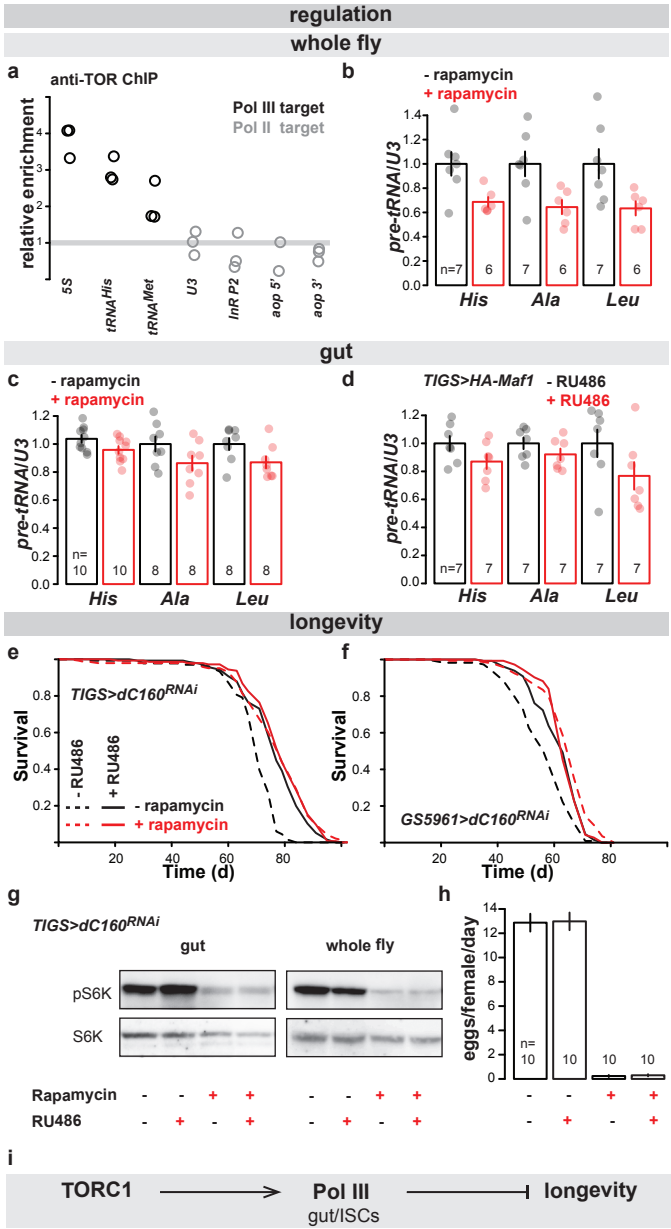
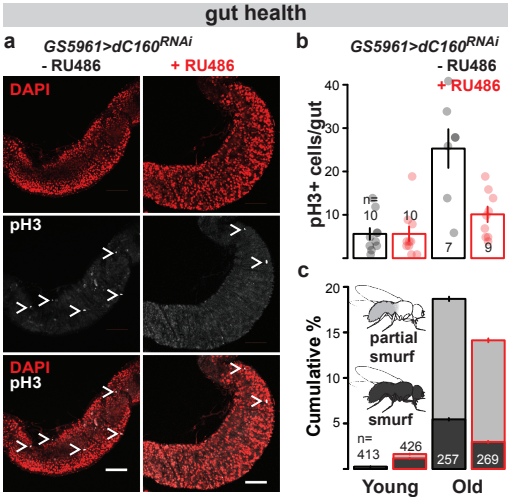
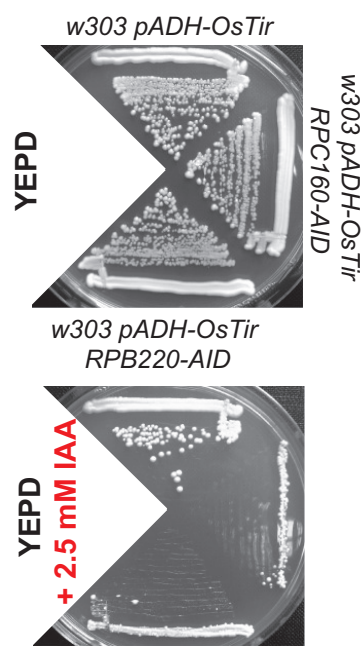


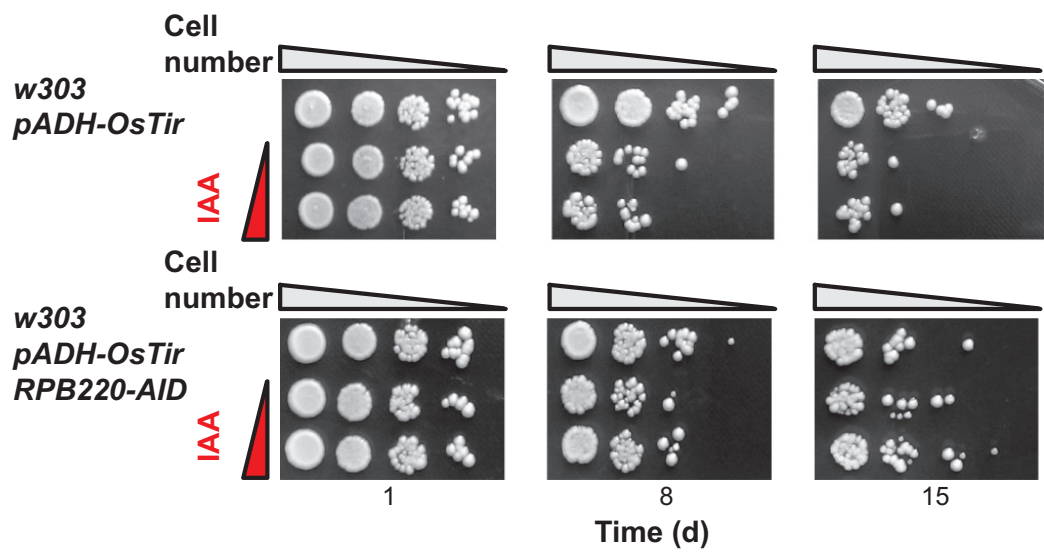
Fig. 4



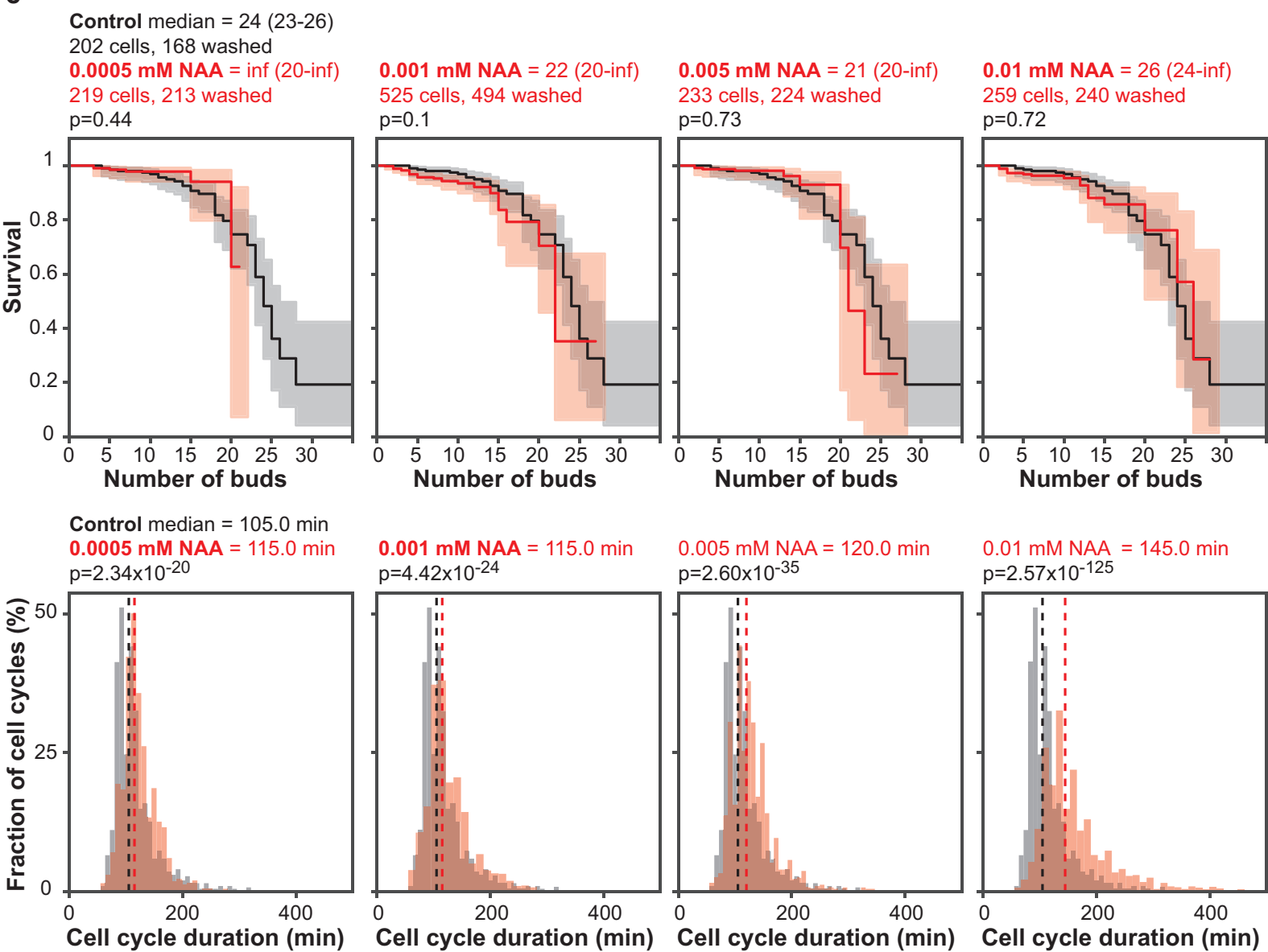
a

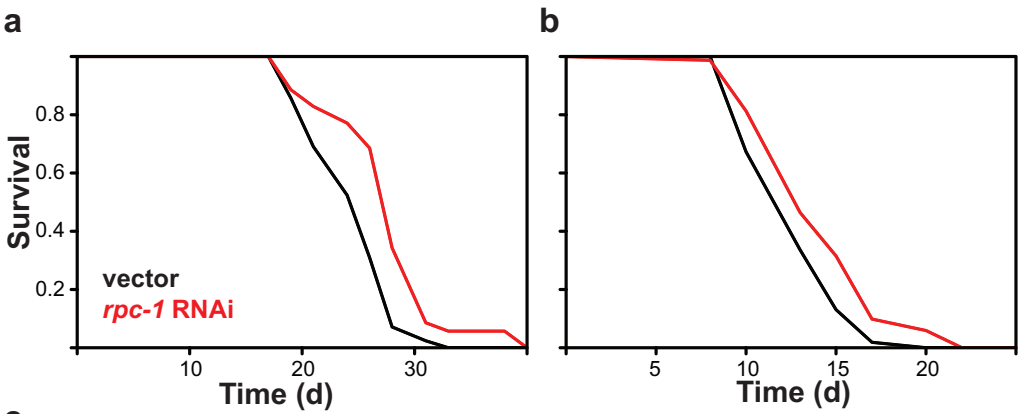


b



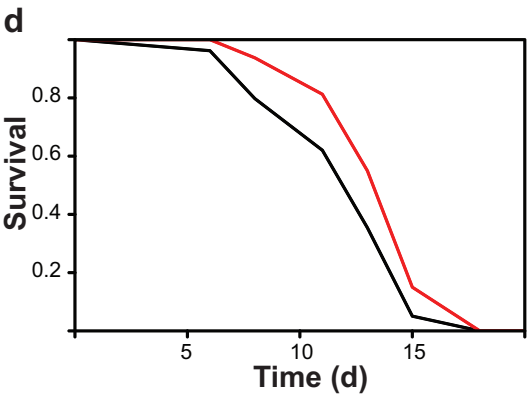
c





c

Strain	<i>rpc-1</i> RNAi	FUDR	Temp	Mean	Dead	Censored	<i>p</i>
N2	-	+	25°C	13.01	54	6	0.009
	+	+	25°C	14.31	62	15	
N2	-	+	25°C	14.09	85	42	0.002
	+	+	25°C	15.55	101	42	
N2	-	+	20°C	20.72	59	41	<0.001
	+	+	20°C	28.14	22	78	
N2	-	+	20°C	21.86	48	52	<0.001
	+	+	20°C	27.10	29	71	
N2	-	+	20°C	21.96	52	34	0.032
	+	+	20°C	24.67	21	73	
N2	-	-	20°C	24.71	42	58	<0.001
	+	-	20°C	27.77	35	65	
N2	-	-	20°C	24.67	26	74	0.002
	+	-	20°C	29.43	23	77	
VP303	-	+	20°C	16.89	52	38	0.024
	+	+	20°C	18.92	29	38	
VP303	-	+	20°C	16.36	57	27	<0.001
	+	+	20°C	19.06	50	56	
VP303	-	+	25°C	12.48	78	6	0.009
	+	+	25°C	13.86	97	6	
VP303	-	+	25°C	12.42	79	0	0.001
	+	+	25°C	13.99	80	3	



Yeast gene	<i>Drosophila</i> orthologue
<i>RPC160 (RPO31)</i>	<i>CG17209</i>
<i>RPC128 (RET1)</i>	<i>RpIII128</i>
<i>RPC82</i>	<i>CG12267*</i>
<i>RPC53</i>	<i>CG5147</i>
<i>RPC37</i>	<i>Sin</i>
<i>RPC34</i>	<i>CG5380</i>
<i>RPC31</i>	<i>CG33051*</i>
<i>RPC25</i>	<i>CG7339</i>
<i>RPC17</i>	<i>Rcp†</i>
<i>RPC11</i>	<i>CG33785</i>

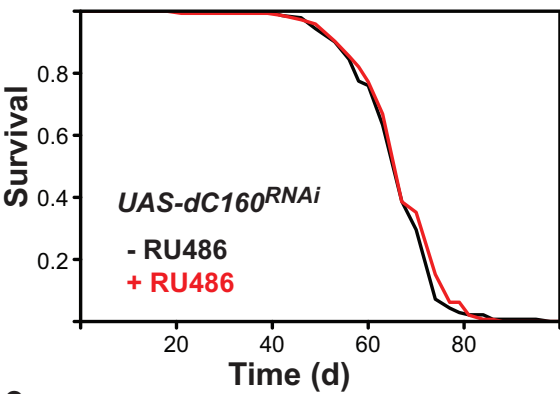
* - identified by homology to the human orthologue

† - low confidence hit identified by homology to the human orthologue

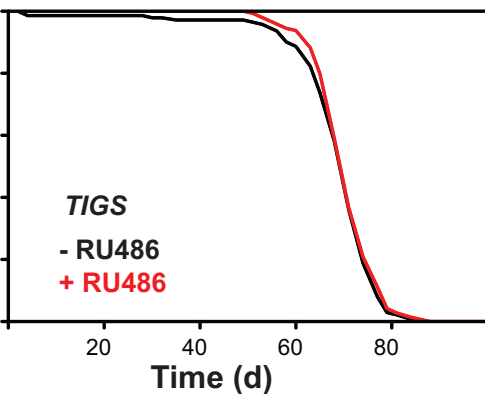
a

Genotype	RU486	Dead	Censored	Median	p
<i>wt</i>	NA	152	0	57	
<i>dC53^{EY/+}</i>	NA	143	1	63.5	6.1x10 ⁻¹³
<i>TIGS>dC53^{RNAi}</i>	-	140	3	69.5	
	+	115	24	72.5	3.1 x10 ⁻⁶
<i>TIGS>dC160^{RNAi}</i>	-	149	1	71	
	+	155	2	79.5	6.4x10 ⁻¹⁶
<i>TIGS>dC160^{RNAi}</i>	-	119	2	65	
	+	134	0	70.5	5.9x10 ⁻⁷
<i>TIGS>dC160^{RNAi}</i>	-	140	2	64.5	
	+	152	0	69	1.8x10 ⁻¹³
<i>TIGS>dC160^{RNAi} males</i>	-	137	4	57	
	+	137	2	59	0.033
<i>GS5961>dC160^{RNAi}</i>	-	138	1	61.5	
	+	139	3	71	2.3x10 ⁻⁴
<i>GS5961>dC160^{RNAi}</i>	-	113	0	57	
	+	130	0	60.5	1.5x10 ⁻⁵
<i>GS5691>dC160^{RNAi}</i>	-	138	3	64.5	
	+	131	1	68.5	1.0x10 ⁻³
<i>TIGS</i>	-	140	1	69.5	
	+	144	1	69.5	0.41
<i>GS5961</i>	-	88	1	68.5	
	+	87	4	68.5	0.88
<i>UAS-dC160^{RNAi}</i>	-	141	1	65	
	+	145	1	65	0.28
<i>S₁₁₀₆>dC160^{RNAi}</i>	-	158	0	75.5	
	+	154	1	75.5	0.21
<i>elavGS>dC160^{RNAi}</i>	-	147	1	75.5	
	+	155	0	78	0.026
<i>TIGS>HA-Maf1</i>	-	150	3	63	
	+	142	4	65	0.006

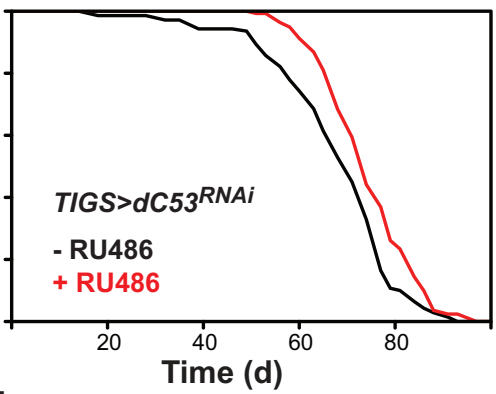
b



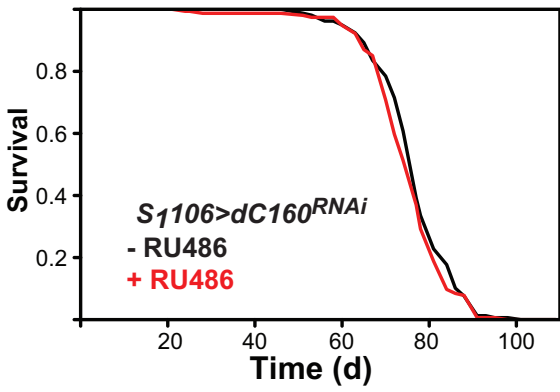
c



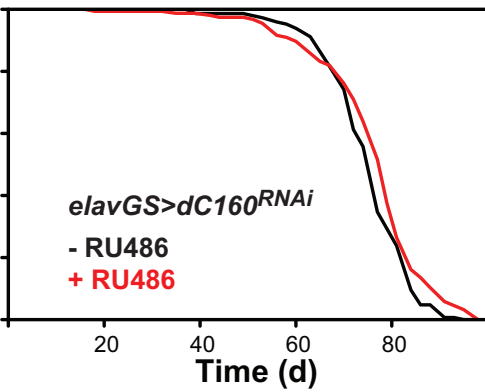
d



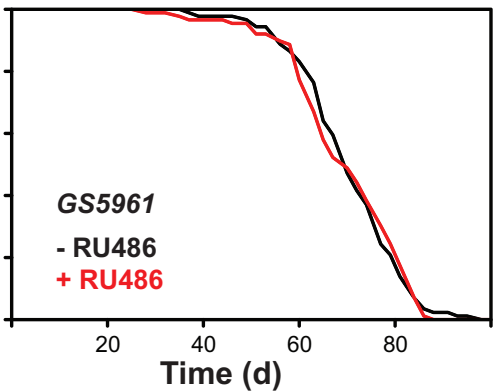
e



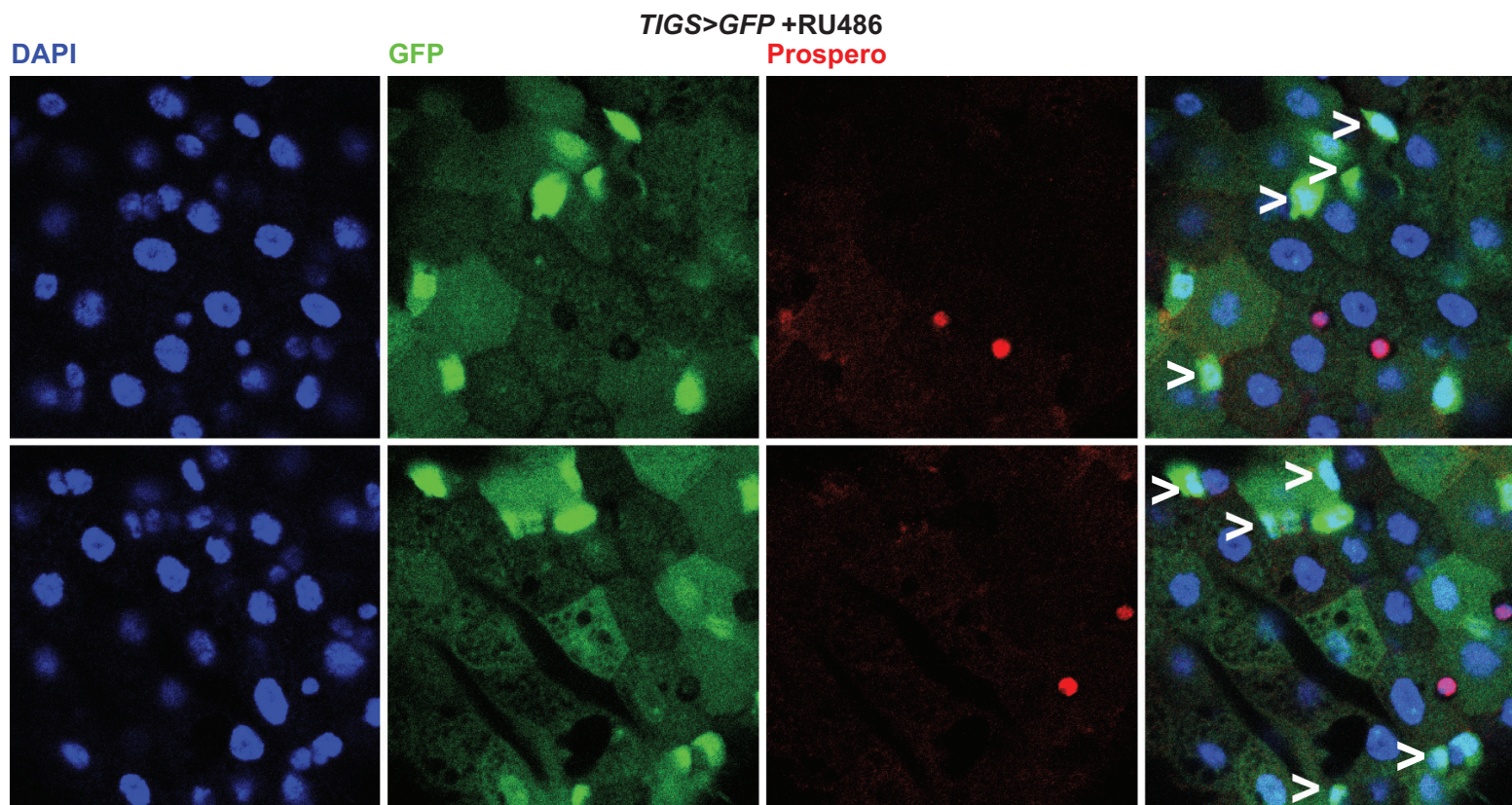
f



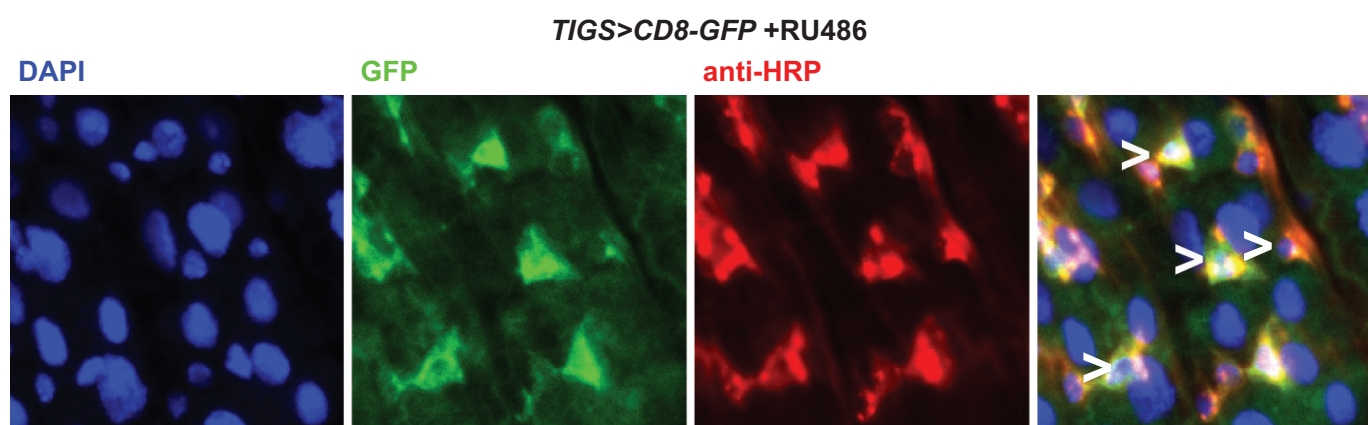
g

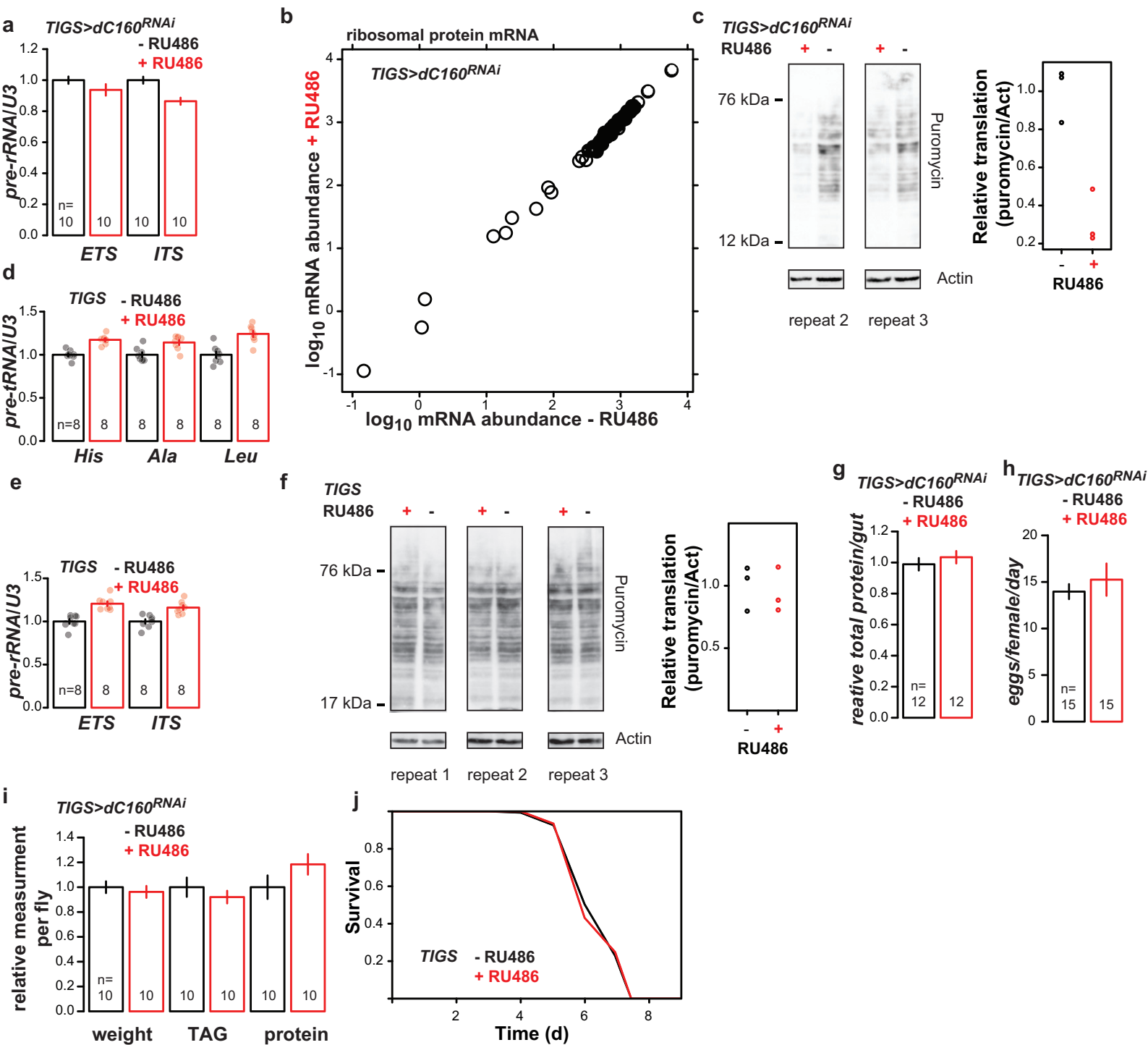


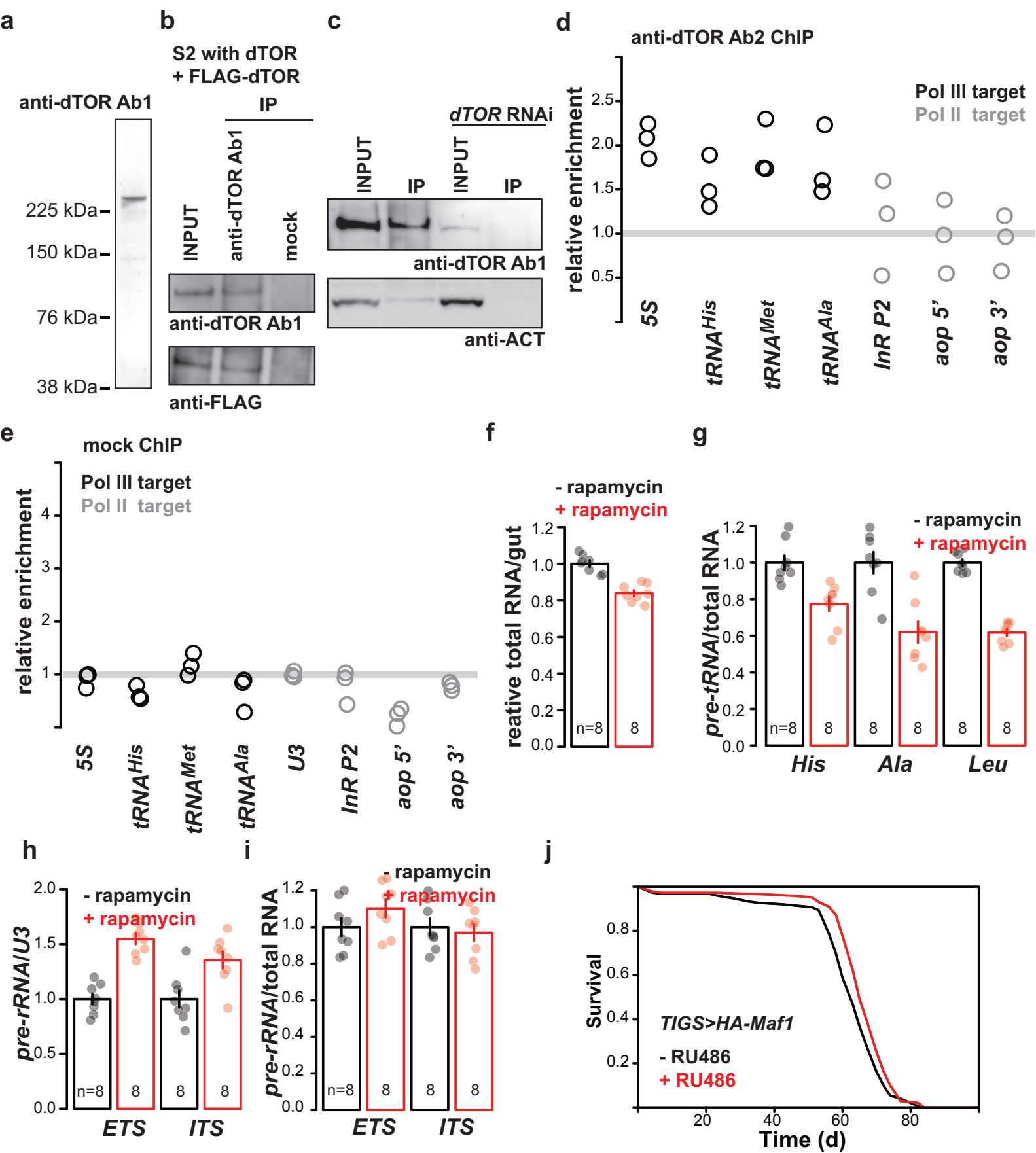
a

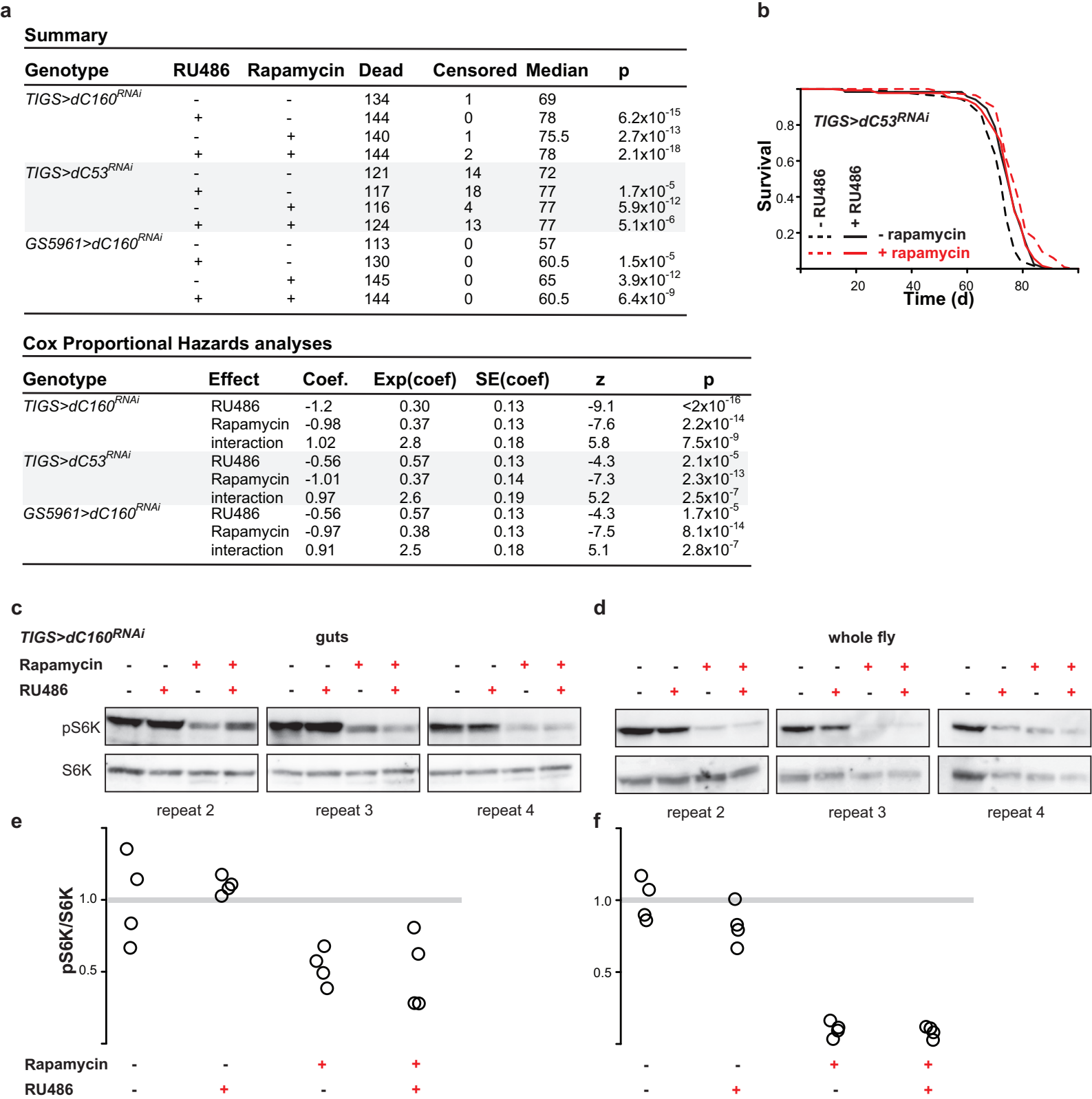


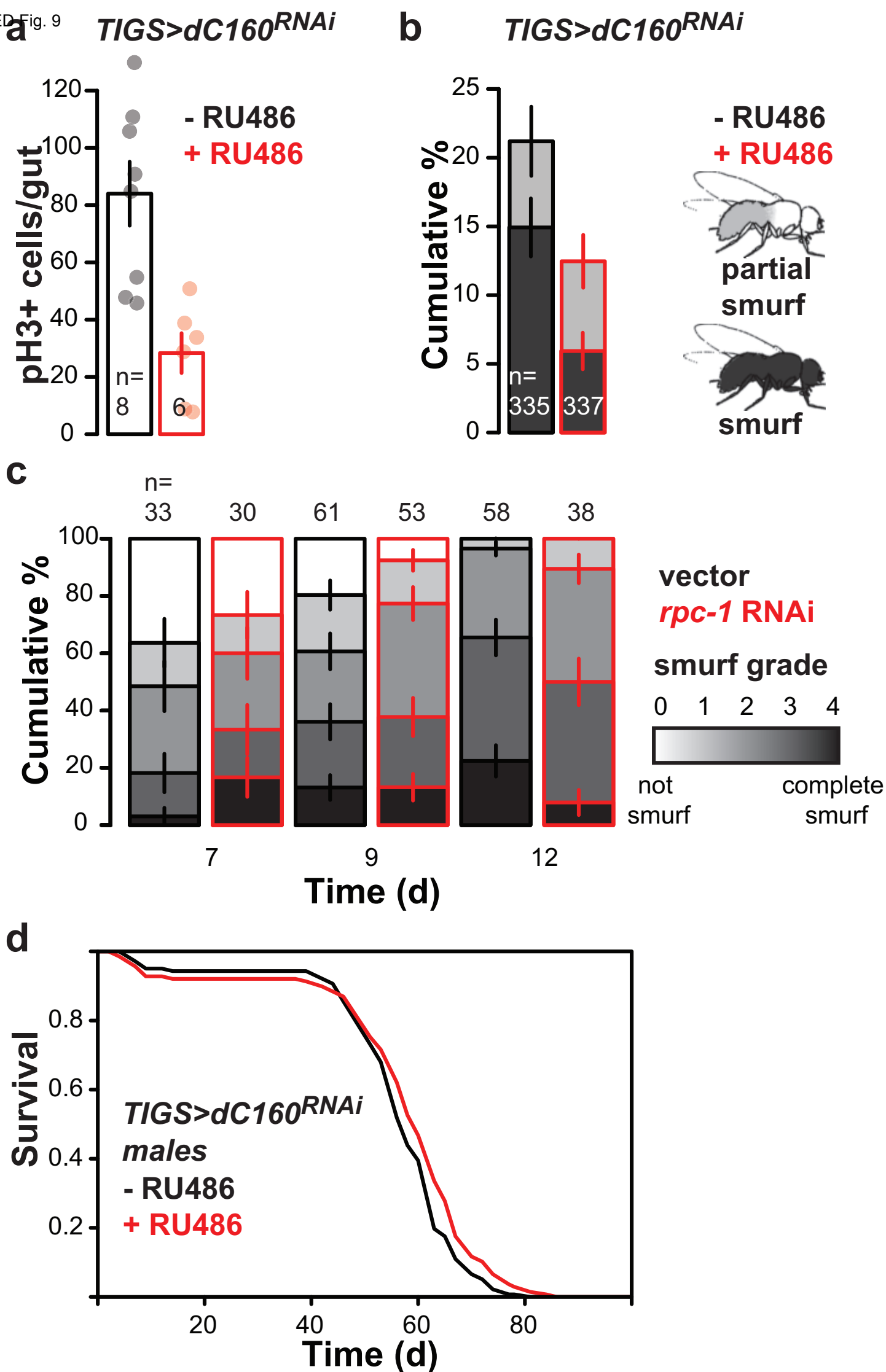
b











1 **SI Guide**

2

3 Supplementary Figure 1 – source data for gels. Single pdf.

Sup. Fig. 1

